Weldability of Li-b aring aluminium alloys

A. Kostrivas and J. C. Lippold

Lithium bearing aluminium alloys constitute a relatively new generation of high performance, lightweight aviation alloys that are being considered for a variety of applications requiring welded construction. As with other aluminium alloys, there are a number of weldability issues associated with these alloys, including resistance to defect formation during fabrication, mechanical property degradation, and service performance. This report reviews the pertinent literature regarding the welding characteristics, properties, and weldability of a number of commercial alloys. The review is divided into the following major sections: (1) development and physical metallurgy of Al–Li–X alloys, (2) microstructure evolution, (3) mechanical properties, (4) weld cracking susceptibility, (5) porosity formation and prevention, and (6) corrosion behaviour. The commercial Al–Li–X alloys are welded using a variety of processes, including arc welding, high energy density welding, and solid state welding. The strength of welds in these alloys varies widely, depending on the welding process, filler metal selection, and post-weld heat treatment. In general, these alloys have low joint efficiency (ratio of weld strength to base metal strength) in the as welded condition and require post-weld aging to achieve efficiencies substantially above 50%. Weld porosity has been a particular problem with these alloys in part due to the hygroscopic nature of Li-containing aluminium oxides. This problem can be controlled if proper surface preparation and cleaning procedures are used. The Al–Li–X alloys tend to be more susceptible to weld solidification cracking than comparable alloys without Li additions. Basic weld solidification theory is used to explain this increase in susceptibility. Some of these alloys exhibit an unusual fusion boundary cracking phenomenon that is associated with an equiaxed grain zone that forms via a solidification mechanism in alloys containing Li and Zr. IMR/330

 The authors are in the Welding and Joining Metallurgy Group, Department of Industrial, Welding, and Systems Engineering, The Ohio State University, Columbus, OH, USA.

Introduction

The most relevant publications accounting for the weldability of commercial and near commercial Al–Li–X alloys are reviewed. Alloys referenced herein are the Soviet alloy 01420, the early developed 2020 as well as 8090, 2090, 2091, and the newly developed Weldalite 049 family (2094, 2095, 2195).[1–11]

Aluminium–lithium alloys initially were not designed with weldability in mind with the exception of the Weldalite 049 alloys,[5,10] since mechanical fastening was the primary joining process in aerospace applications. However, riveting is a tedious operation, unhealthy for the operator,[11] and very slow due to the large number of bolted and riveted joints. On the other hand, welded structure gives weight savings (elimination of rivets, sealants, rubbers, and glues), less use of labour in manufacture, and reliability in performance due to uniform distribution of stresses in joint elements as compared with riveted or bolted joints.[12] For these alloys to have an extended use in a wider range of applications, weldability should be studied and potentially more weldable alloy variants should be developed.

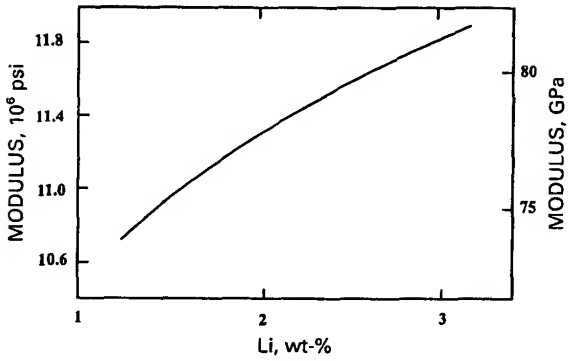

1 Elastic modulus of Al–Mg–Li alloys *v.* lithium content[4]

The current review aims at providing a general description of the physical metallurgy of the alloys mentioned above together with issues that potentially compromise their weldability. Therefore, mechanical property degradation in both the weld region and heat affected zone (HAZ) is addressed along with weld porosity, solidification cracking susceptibility, and liquation cracking susceptibility. Resistance to corrosion coupled with alloy composition and heat treatment is also reviewed.

Classification and physical metallurgy of Al–Li–X alloys

Lithium-bearing aluminium alloys constitute a group of high performance wrought aluminium alloys intended for use principally in aircraft and aerospace structures. Reduced density and increased elastic modulus coupled with very good cryogenic toughness and ductility (Table 1) make Li-bearing aluminium alloys an attractive alternative relative to more conventional precipitation hardenable aluminium alloys (e.g. 2024, 2014, 2219, 6061, and 7075).[1–9]

It is known that every 1 wt-%Li in aluminium decreases the density[4–6] by about 3% and increases the elastic modulus E by about 6%. Figure 1 shows that effect for Al–Mg–Li alloys. Pickens in his review paper[4] states that for an Al–Li* alloy, structural weight savings would be in the range between 10 and

* All compositions are in weight-% unless otherwise stated.

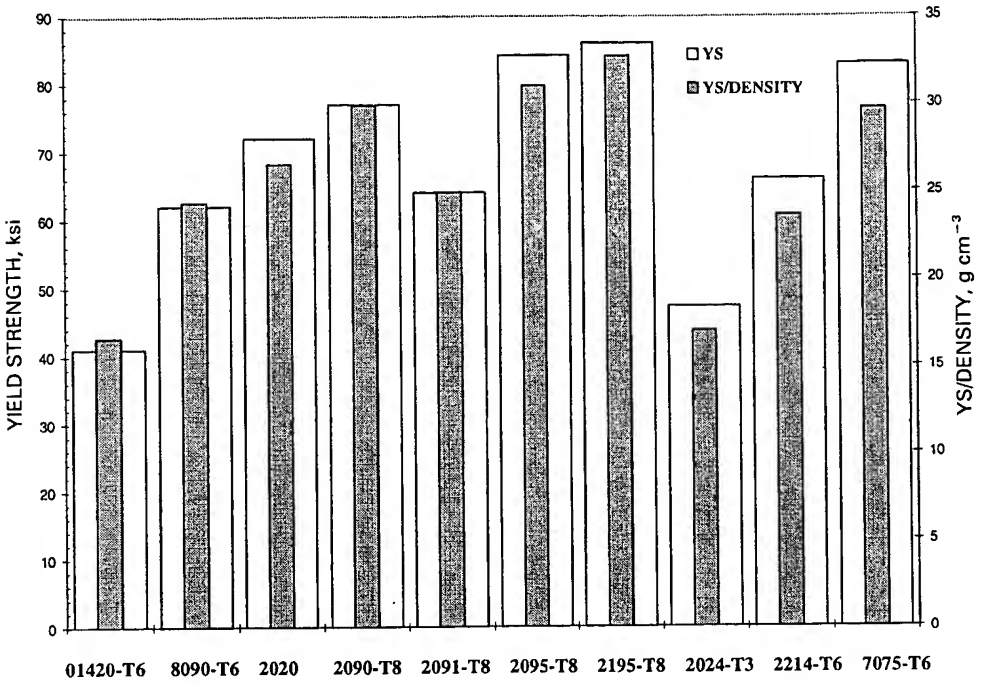

1 ksi ≈ 6·9 MPa

2 Yield strength (YS) and YS/density ratio for various Al alloys[3,4,7,9]

16%. Figure 2 illustrates the yield strength/density ratio for some commercial Al–Li–X alloys as well as the same ratio for some conventional aerospace Al alloys.

Such a weight reduction could be cost effective even when compared with composite materials considering that they have high production costs.[7] Composites are being used extensively in certain areas of high performance aircraft offering potential weight savings of about 25% compared with that achievable by conventional aluminium alloy products.[8] However, Li-bearing aluminium alloys appear to be competitive alternatives.

Classification

Despite the difficulties in the production of Li-bearing aluminium alloys due to the high reactivity of Li, alloys were produced as early as the 1920s in Germany.[6] Further improvements in alloy processing techniques enabled the production of a range of Li-bearing aluminium alloys.[8] Today's commercial or near commercial alloys[3] can be divided into four major groups, namely, Al–Mg–Li and Al–Cu–Li ternary alloys, and Al–Cu–Li–Mg and Al–Li–Cu–Mg quaternary alloys. The commercial alloys that fall within each of these groups are shown in Fig. 3. The

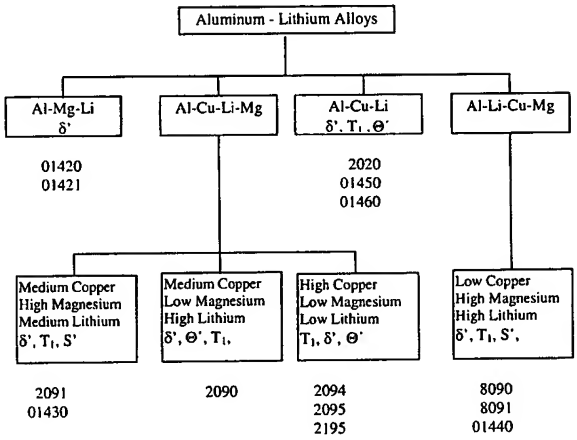

3 Ternary and quaternary aluminium alloy systems containing lithium, showing commercial alloy designations and primary strengthening precipitates[3,13–15]

nominal compositions of the specific alloys are listed in Table 2. Minor additions of other elements such as Zr and Mn are used to modify microstructure and as a result the mechanical properties of Al–Li–X alloys but these effects are discussed below.

Table 1 Cryogenic properties of high strength alloy 2090 (Ref. 9)

Test temperature		UTS, ksi (MPa)		YS, ksi (MPa)		Elongation, %		K_{IC}, ksi in$^{1/2}$ (MPa m$^{1/2}$)	
°C	°F	L	LT	L	LT	L	LT	L–T	T–L
25	77	81·9 (565)	81·9 (565)	77·6 (535)	77·6 (535)	11·0	5·5	30·9 (34)	22·7 (25)
−196	−320·8	103·7 (715)	100·8 (695)	87·0 (600)	90·6 (625)	13·5	5·5	47·3 (52)	30·9 (34)
−269	−452	119 (820)	118 (818)	89·2 (615)	102 (705)	17·5	6·5	59·1 (65)	35·5 (39)

*L longitudinal; LT long transverse; L–T fracture toughness in longitudinal direction; T–L fracture toughness in long transverse direction.

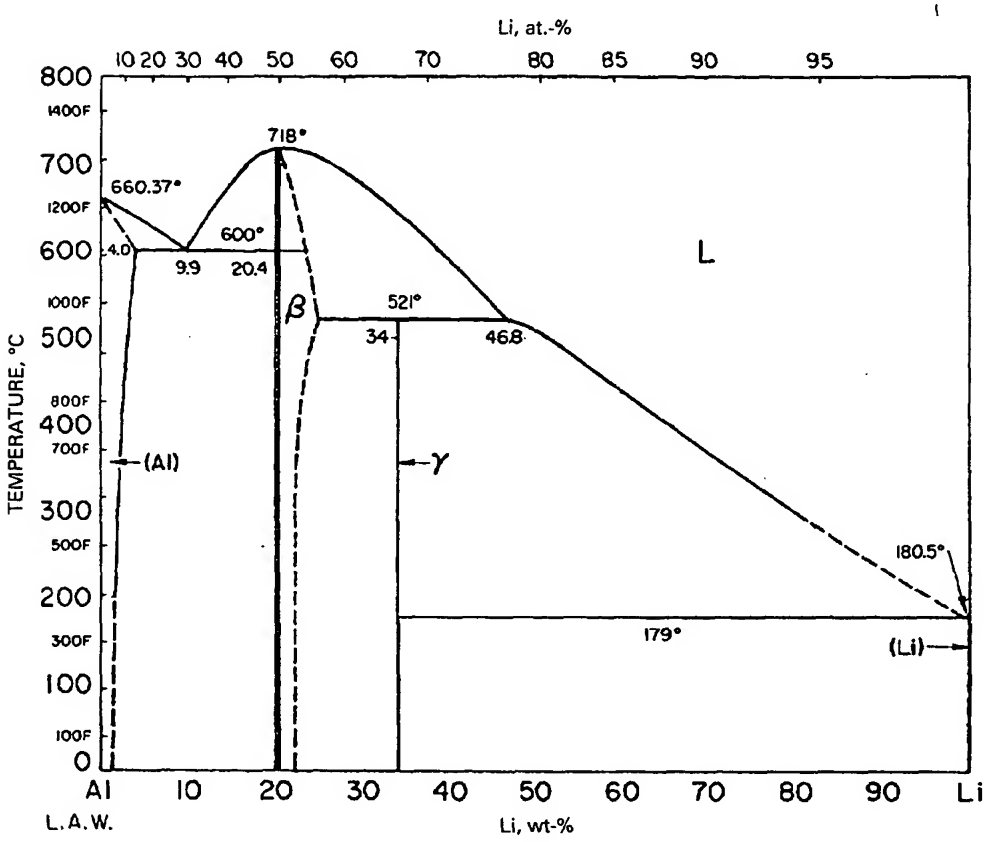

4 Binary phase diagram for Al–Li system[20]

Physical metallurgy

Binary Al–Li alloys

The Al–Li phase diagram[19] is shown in Fig. 4. The limited solid solubility of Li in Al (~4 wt-% at 600°C, <1 wt-% at 100°C) makes strengthening of this binary alloy system possible via precipitation reactions. Metastable δ'-Al_3Li phase (Fig. 5) is the primary strengthening precipitate and is considered to be coherent with the matrix[20] phase since its lattice parameter is close to that of aluminium and hence results in low misfit strain and coherency with the matrix. The maximum solvus temperature for the phase δ' is 300–350°C at ~14 at.-%Li (~4 wt-%Li).

On aging following a solution heat treatment, δ' precipitates homogeneously in the form of spheres.[6] The precipitation sequence can be described as

$$\alpha_{\text{solid solution}} \rightarrow \alpha + \delta' + \delta \rightarrow \alpha + \delta$$

where δ is the equilibrium phase (AlLi).

Overaging results in formation of the δ-phase. The transformation $\delta' \rightarrow \delta$ is likely to occur by δ' dissolution and subsequent δ precipitate formation.

Table 2 Nominal compositions (wt-%) and typical mechanical properties of commercial Al–Li alloys[3–5,7,16–18]

Alloy	Li	Cu	Mg	Zr	Other	Yield strength*, ksi	Ultimate strength*, ksi
01420-T6	2·0	...	5·3	0·10	0·5Mn	41	67
01421-T6	1·9	...	5·0	0·08	0·17Sc	52	70
01430	1·7	1·6	2·7	0·11	...	54	67
01440	2·3	1·5	0·9	0·15	...	56	70
01441	1·9	2·0	0·9	0·09	0·05Be, 0·11Fe	...	72
01450	1·9	3·15	...	0·10	0·08Ti	71	84
01460	2·1	3·1	...	0·09	0·075Sc	67	75
8090-T8	2·5	1·0	1·0	0·10	...	70	77
8091-T8	2·6	1·9	0·9	0·12	0·1Fe, 0·1Si	78	84
2020-T6	1·2	4·4	...	...	0·5Mn, 0·2Cd	77	82
2090-T8	2·3	2·7	0·2	0·12	...	75	81
2091-T8	2·0	2·2	1·5	0·10	...	64	70
Weldalite 049-T8	1·3	5·4	0·4	...	0·04Ag	101	104
2094	1·3	4·7	0·4	0·14	0·4Ag	...	...
2095-T8	1·0	4·0	0·4	0·14	0·4Ag	84	90
2195-T8	1·0	4·0	0·4	0·12	0·4Ag	86	90

* 1 ksi ≈ 6·894 MPa.

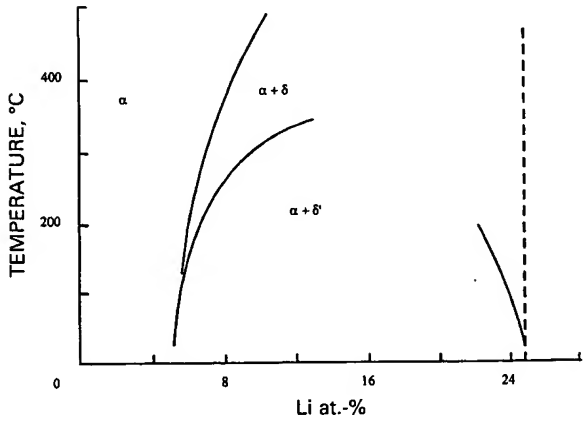

5 Lower part of Al–Li binary system[21]

Although δ' precipitates result in high strength they are considered to be detrimental to ductility and fracture toughness since δ' particles can be sheared by dislocations.[18,22]

All the Li-bearing alloys are strengthened to some degree by precipitation. In some alloys, multiple precipitates may be present and/or complex precipitation sequences used to optimise strength, ductility, toughness, and fatigue resistance. For easy reference, these precipitates are listed in Table 3.

Al–Mg–Li(–Zr) alloys

Alloy 01420 is the product of many years of Russian development[4] and was employed in the construction of the welded supersonic aircraft[11,12] MIG–29. It has a nominal composition Al–5Mg–2Li–0·1Zr. Additions of Mg to the Al–Li binary system result in lower solid solubility of Li in aluminium.[31] The reduced solubility of Li in the matrix yields a higher volume fraction of δ' which contributes to higher levels of strength. Since alloy 01420 does not contain Cu it possesses low density[12] (2·47 g cm^{-3}). In addition, Mg does not form precipitates (with the exception of Al_2MgLi on overaging) due to its high solubility limit. However, its contribution to the strength of the alloy is via solid solution. The precipitation reaction can be described as

$$\alpha_{\text{solid solution}} \rightarrow \alpha + \delta' \rightarrow \alpha + \delta + (Al_2MgLi)$$

Al_2MgLi is a product of extended aging and adversely affects alloy strength, ductility, and toughness. Formation of Al_2MgLi phase within the matrix also promotes precipitation in the precipitation free zones (PFZs) which are narrow regions along high angle boundaries associated with poor ductility and fracture properties.[18] Precipitation free zones are regions where precipitate nucleation is difficult due to vacancy and/or solute atom depletion since they are lost to the nearby sinks.[32] Vacancy–solute binding energies, degree of initial supersaturation, and subsequent thermomechanical treatments determine the extent of the formation of PFZs. The effect of those PFZs on alloy properties such as stress corrosion cracking (SCC) are discussed below.

Zr additions

Zirconium has low solubility in the aluminium alloy and, as a result, a fine dispersion of metastable β' [Al_3Zr] and/or α' [$Al_3(Zr,Li)$] spherically shaped particles is formed.[21] These precipitates inhibit recrystallisation and promote grain refinement. It is stated that zirconium intermetallics are considerably finer than manganese intermetallics and are distributed within the matrix with greater density providing more effective strengthening.[15,33] The β' precipitates also serve as heterogeneous nucleation sites for δ' [Al_3Li] while β' particles also resist dislocation cutting due to a high antiphase boundary energy. Precipitation free zones are strengthened due to β' precipitation.[3,18]

Strengthening phases in Al–Cu–Li alloys

The precipitation reactions are quite complex in this system. The precipitation sequence can be described as follows:

$$\alpha_{\text{solid solution}} \begin{cases} \rightarrow \text{GP zones} \rightarrow \Theta' \begin{cases} \rightarrow \Theta' \rightarrow \Theta\ (Al_2Cu) \\ \rightarrow T_1\ (Al_2CuLi) \end{cases} \\ \rightarrow \delta' \rightarrow \delta \end{cases}$$

Copper reduces the solubility of Li in aluminium while Li modifies the structure of GP zones and also affects precipitation of the Θ'' and Θ' phases.[18,20] The primary strengthening phases present seem to be a

Table 3 Precipitation in Li-bearing aluminium alloys[20,23–30]

Precipitate	Stoichiometry	Crystal structure	Alloys
δ	AlLi	B32 (cubic)	01420, 01421, 01430, 01440, 01450, 01460, 2090, 2091, 2094, 2095, 2195, 8090, 8091
δ'	Al_3Li	L12 (ordered fcc)	
Θ'	Al_2Cu	Tetragonal	01450, 01460, 2020, 2090, 2094, 2095, 2195
Θ	Al_2Cu	bct (C16)	
T_1	Al_2CuLi	Hexagonal	01450, 01460, 2020, 2090, 2094, 2095, 2195, 8090
T_2	Al_6CuLi_3	Icosahedral, group M35	2020, 2091
T_B	$Al_{15}Cu_8Li_2$	fcc (C1)	2020
S'	Al_2CuMg	Orthorhombic	01430, 01440, 2090, 2091, 2094, 2095, 2195, 8090, 8091
S	Al_2MgLi	Cubic	01420, 01421
α'	$Al_3(Zr_{1-x},Li_x)$	L12 (ordered fcc)	01420, 01421, 01430, 01440, 01450, 01460, 8090, 8091, 2090, 2091, 2094, 2095, 2195
β'	Al_3Zr	L12 (ordered fcc)	
β'_{Sc}	$Al_3(Zr_x,Sc_{1-x})$	L12 (ordered fcc)	01421, 01460

function of the Cu content and are briefly described for the following alloy systems.

2090 and Weldalite 049 alloys

Alloy 2090 and the Weldalite family alloys have a high copper/magnesium ratio. Strengthening precipitates are Θ', T_1, and δ' while β' particles act as nucleation sites for Θ' in addition to their grain refining role. Precipitation of $T_1[Al_2CuLi]$ phase can be affected by β' dispersoids since they cause retention of the well defined substructure and enhance heterogeneous nucleation.[3,18,20] T_1 is nucleated at subgrain boundaries and on dislocations in the form of platelets.[3,10] Precipitation of T_1 (increase in its volume fraction in the matrix) occurs at expense of Θ' since both phases compete for the available Cu. Increasing volume fraction of T_1-platelet precipitates results in high alloy strength[22] and hence both 2090 and Weldalite alloys possess higher yield strength than other alloys (*see* Table 2). However, increased Cu content results in higher alloy density.

Alloy 2020

The first commercial alloy based on the Al–Cu–Li system was produced by Alcoa in the late 1950s and designated as 2020 by the Aluminum Association. Alloy 2020 possesses high strength, low density (Fig. 2), high elastic modulus, and very good corrosion properties, which made it attractive for use in high performance military structures such as the US Navy's A–5A and RA–5C Vigilante[34] airplanes. However, its low ductility and poor fracture toughness led to termination[7] of its production in the late 1960s.

The primary strengthening phases in 2020 are the partially coherent $\Theta'(Al_2Cu)$, $T_1(Al_2CuLi)$, and $T_B(Al_{15}Cu_8Li_2)$.[20] TEM studies reveal that Θ' is significantly more prominent[35,36] than either T_1 or T_B. Cadmium suppresses Θ'' precipitation, aids nucleation of Θ', and inhibits grain and precipitate growth by segregating to the Θ'/matrix interface.[37,38] Manganese also inhibits grain growth by forming dispersoids[36] which are present in 2020 as 0·5–1 μm $Al_{20}Cu_2Mn_3$.

Low ductility is suggested to relate to both formation of PFZs due to heterogeneous precipitation of equilibrium phases along grain boundaries and metastable coherent δ' (Al_3Li) and partially coherent T_1 precipitates which form on aging. For aging conditions that do not produce PFZs cracking occurs within the grains due to shearing of coherent and partially coherent precipitates by moving dislocations. When PFZs are present, cracking occurs due to plastic deformation in these soft regions[39,40] and cracks propagate intergranularly (or just adjacent to the grain boundary in the PFZ). Cadmium segregation is likely to enhance crack propagation along grain boundaries by lowering the surface energy associated with fracture.[36]

2091 and 8090 alloys

These alloys have a low copper/magnesium ratio and consequently Θ' is not a significant strengthening precipitate. The S' phase (Al_2CuMg) is favoured and strength is lower compared with that of the Weldalite alloys. The S' promotes cross-slip, improves ductility and toughness, but reduces fatigue resistance. Equilibrium δ-phase does not seem to form in alloys with a higher magnesium content, and is generally not observed in these alloys.

Other strengthening phases are δ' and T_1. The latter competes with S' for available Cu atoms and heterogeneous nucleation sites.[18] Straining (or stretching) of wrought alloys before aging provides new heterogeneous nucleation sites and therefore eliminates T_1 and S' PFZs.

Scandium additions

Small additions of scandium together with Mg seem to increase the strength of Al–Cu–Li alloys,[41] aged in the temperature range 20–180°C. Increase in strength is due to grain and subgrain refinement and a higher density of β'_{Sc}-$Al_3(Zr,Sc)_X$ dispersoids. It is important to note that due to lower diffusion coefficients of both Sc and Zr, the distribution of the dispersoids is primarily dependent on the distribution of these elements in the matrix of the cast alloy.[33] Scandium also promotes refinement of δ' and T_1 precipitates which results in good alloy ductility in addition to enhanced strength properties.[41] Formation of layered particles was also observed with the addition of Sc. In the case of Al–Mg–Li–Zr alloys, δ' was found[42] to precipitate and form a shell around the β'_{Sc} particle. Aging in the temperature range between 140 and 170°C caused thickening of this shell and increased the strength of the alloy.

Alloying of the Al–Mg–Li system with Sc has been reported to promote an improvement of alloy resistance to overaging in the HAZ as compared with the 01420 Soviet alloy.[43] This means that Sc-bearing alloys are relatively insensitive to prolonged heating at 300–350°C and their hardness remains essentially unchanged. Fridlyander *et al.*[42] suggest that Al–Mg–Li–Zr–Sc alloys could be considered as a replacement for both 2219 and 01420 commercial weldable alloys. In alloys of the system Al–Mg–Li, scandium decreases the stability of the solid solution in the region of Al_3Mg_2 and $Al_{12}Mg_{17}$ phases. Thereby, segregation of those phases decreases the Mg/Li ratio in the solid solution and decreases its stability in the region of the Al_2MgLi phase at 290°C which causes an overall increase in the strength potential of the alloy.[31] However, the fracture toughness K_{IC} of the alloy through the thickness (short transverse direction) seems to decrease.

Concept of weldability

The term 'weldability' refers to the ability of a material to be fabricated by welding and for the welded structure to perform satisfactorily in the intended service environment. In order to evaluate a material's overall weldability it is necessary to consider a number of factors. In aluminium alloys four factors typically dictate weldability: (1) mechanical property degradation, or loss of weld joint 'efficiency', (2) susceptibility to cracking during fabrication, usually due to solidification or liquation cracking mechanisms, (3) porosity formation, and (4) resistance to corrosion. Since all these factors are influenced by microstructure, their discussion is prefaced by a section on microstructure evolution.

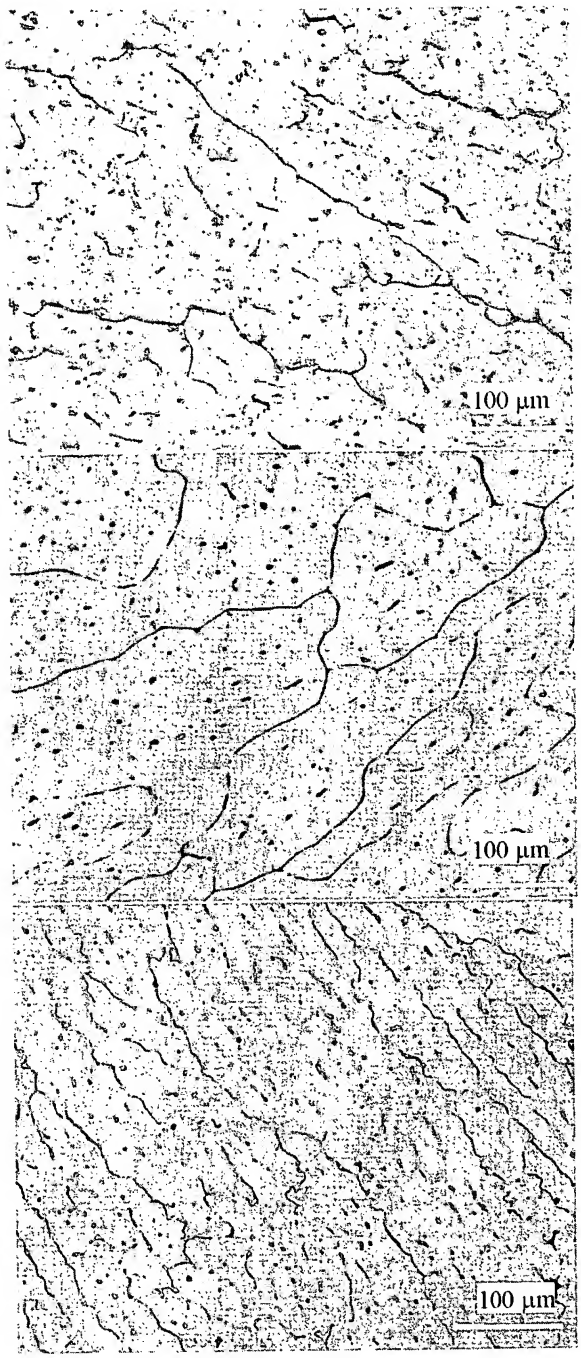

A alloy 2090; *B* alloy 8090; *C* alloy 2195

6 Representative fusion zone microstructure of autogenous welds, Barker's etch

Microstructure evolution

A typical fusion weld contains a number of distinct regions that can broadly be classified as a fusion zone, where melting and resolidification occur, and heat affected zone (HAZ), where the surrounding base metal microstructure is altered by the heat of welding. Fusion zone microstructure in aluminium alloys is primarily dictated by the solidification process, rather than by post-solidification transformations. During welding, a localised region of the base material is melted and solidified. The solidification morphology,

7 Representative fusion zone microstructure of variable polarity plasma arc welds in 2195 using 2319 filler metal, Keller's etch

as well as the solute distribution, depends on the interrelationship of temperature gradient, solidification growth rate, and diffusion. As a result, different welding processes affect the weld microstructure and subsequent properties differently. For example, high energy density processes like electron beam welding (EBW) produce refined weld metal microstructures while arc welding processes such as gas tungsten arc welding (GTAW) result in coarser microstructures. Strengthening of the fusion zone by aging following welding is limited since much of the solute needed to form precipitates is tied up in a eutectic constituent, which forms at the end of solidification.[44]

Figure 6 shows the fusion zone microstructure of autogenous gas tungsten arc (GTA) welds in alloys 2090, 8090, and 2195, while Fig. 7 shows the microstructure of a variable polarity plasma arc weld in alloy 2195 using 2319 filler metal. As described in a subsequent section, non-equilibrium weld solidification conditions promotes the formation of some eutectic in the fusion zone during the final stages of solidification in all the Al–Li–X alloys. As a result, the predicted solidification temperature range is the difference between the equilibrium liquidus temperature and the eutectic temperature.

Microstructure within the HAZ is primarily dictated by solid state reactions that occur in regions heated to elevated temperature as heat flows away from the fusion zone. In the Li-bearing aluminium alloys, most HAZ microstructural changes are associated with an alteration of the strengthening precipitates. Other changes, such as grain growth, may also occur, but their effect on HAZ properties is relatively minor.

Coarsening of precipitates is anticipated to be limited to locations experiencing relatively low peak temperatures whereas precipitate dissolution seems to take place at regions experiencing higher peak temperatures. It is difficult to produce a quantitative analysis of the HAZ of alloys possessing a variety of strengthening precipitates since one phase may dissolve while another coarsens. Both dissolution and coarsening are primarily diffusion controlled

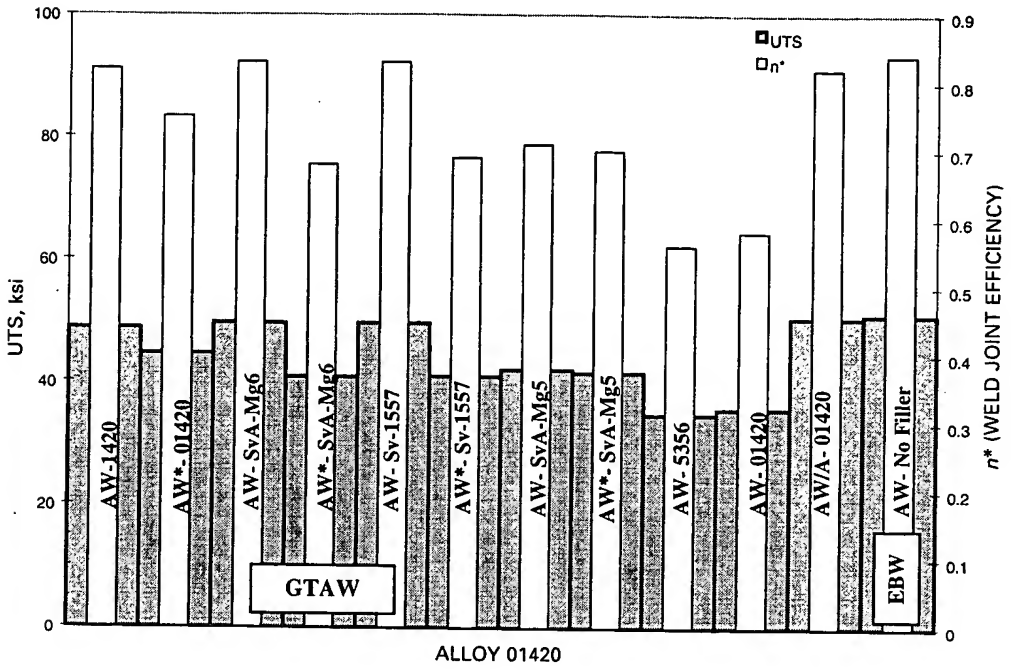

AW:As Welded, AW*:As Welded/Reinforcement Removed, AW/A: Postweld Aged
AW/ST/A: Postweld Solution Treated and Aged
n*= Weld UTS/BM UTS

8 Weld joint strength and efficiency for Soviet 01420 alloy using various processes and filler metals[2–5]

processes. The stability of the various precipitates described above, at elevated temperatures depends on the ability to minimise the free energy of the system, namely, the minimisation of chemical free energy which is the driving force for dissolution and the reduction of the interfacial energy which takes place with precipitate coarsening.[45]

Dissolution of precipitates close to the fusion boundary provides solute in the matrix and results in increased strength of the alloy due to solid solution strengthening but the overall increase of strength in these regions stems from reprecipitation during cooling from elevated temperature. Regions where partial dissolution exists have lower strength due to lower fraction of precipitation whereas regions experiencing lower temperatures possess lower strength due to the precipitate coarsening effect.[22,46]

Mechanical properties

Precipitation hardenable aluminium alloys exhibit lower tensile strength and ductility in the as welded condition. In general, improvement in the weld fusion zone integrity can be accomplished by modifying the composition and microstructure through the proper selection of filler metals and welding parameters.[44] However, the thermal cycles in the HAZ can promote complex metallurgical reactions as described above and corresponding microstructural and mechanical property changes in the optimal heat treated base metal.[3,22] Consequently, a reduction in mechanical properties occurs in the HAZ, particularly in regions close to the fusion boundary. The HAZ properties cannot be easily recovered without complete solution treatment and aging. However, such a procedure cannot be applied in all cases, particularly in those that involve large components. As a result, as welded properties are frequently limited by alloy selection and the reduction in HAZ properties is often the limiting factor in determining joint efficiency.

Considerable work has been undertaken to measure and optimise the mechanical properties of a number of commercial alloys, including alloys 01420, 8090, 2090, and Weldalite 049 using matching or near matching filler metals.[2–5,47] Tensile strength and joint efficiency data for the individual alloys are presented in Figs. 8–11.

In general, the as welded joint efficiency (ratio of weld strength to base metal (BM) strength) ranges from 50 to 80%, while Pickens[4] states that efficiencies up to 100% can be achieved for welds that are solution annealed and aged after welding. In the as welded condition, joint efficiencies tend to increase when EBW is used rather than GTAW. This results from the narrower fusion zone and HAZ produced in these welds which allows more constraint from the surrounding base metal.

In the case of alloy 8090 (Fig. 9), improved joint efficiencies with the GTAW process are achieved using solution heat treatment and aging after welding. The highest joint strengths are obtained using 5000 series filler metals, such as 5356, or with a matching filler material (8090). Joint efficiencies are generally lower than those achieved in 01420 alloy welds.

Similar data are compiled in Fig. 10 for alloy 2090 using both the GTAW and EBW processes. The

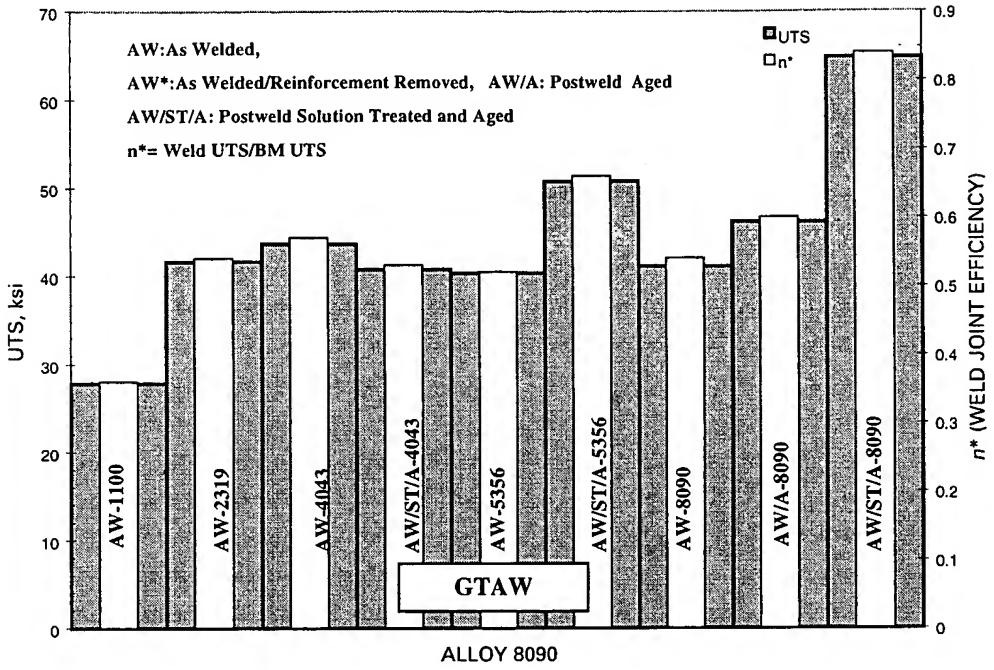

9 Weld joint strength and efficiency for alloy 8090 using various processes and filler metals[2–5]

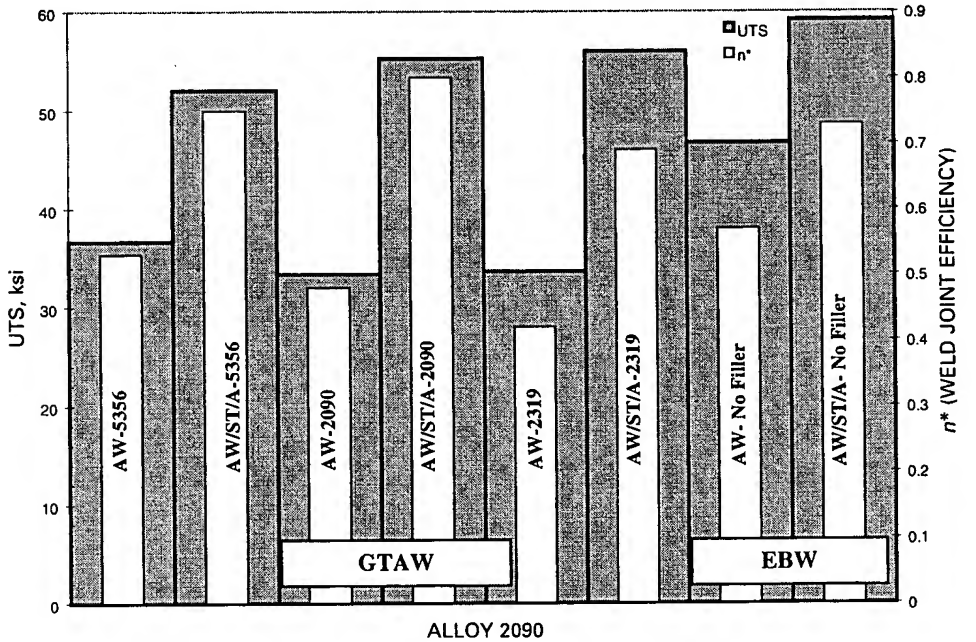

AW:As Welded, AW*:As Welded/Reinforcement Removed, AW/A: Postweld Aged
AW/ST/A: Postweld Solution Treated and Aged
n*= Weld UTS/BM UTS

10 Weld joint strength and efficiency for alloy 2090 using various processes and filler metals[3–5]

tendency towards increased joint efficiency is again apparent when post-weld solution heat treatment and aging are employed. Welds produced with EBW exhibit finer microstructure in the fusion zone and narrower HAZ compared with welds produced using GTAW. By examining weldments of alloy 2090 produced with both GTAW and EBW the degree of solute segregation[48] is more limited in EBW weldments than that produced with GTAW. This distinguishable difference between EBW and GTAW fusion zones affects subsequent solid solution strengthening and aging response. High peak yield strength is obtained for EBW weldments after solution heat treatment and aging due to the availability of

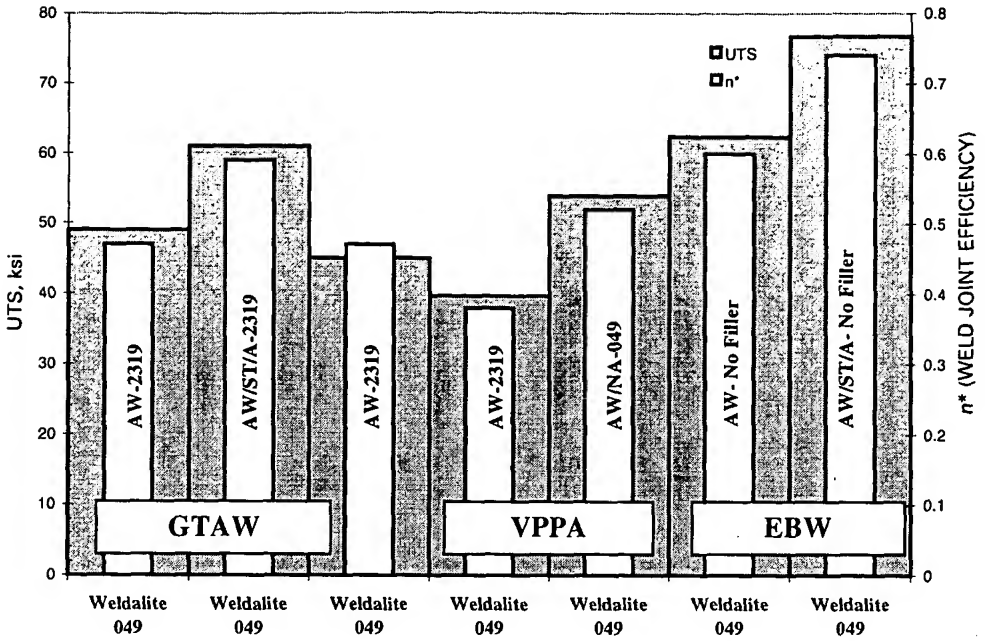

AW:As Welded, AW*:As Welded/Reinforcement Removed, AW/A: Postweld Aged
AW/ST/A: Postweld Solution Treated and Aged
n*= Weld UTS/BM UTS

11 Weld joint strength and efficiency for Weldalite 049 alloy using various processes and filler metals[3–5]

considerable solute in solution within the fusion zone which promotes a stronger and more homogeneous precipitation reaction. GTA weldments do not provide comparable levels of solute for precipitation since the fusion zone contains more eutectic that reduces the overall solute content of the surrounding matrix. As a result, lower yield strengths are realised after post-weld heat treatment and aging.

Both precipitate dissolution and growth are suggested[49] to cause mechanical property degradation in the HAZ of 2090 weldments. Strength recovery in the HAZ after post-weld heat treatment and aging is much improved relative to the fusion zone since no eutectic constituent is present that reduces the matrix solute concentration.

As shown in Fig. 11, Weldalite 049 alloys seem to achieve high strength using filler alloys with increased copper such as 2319 coupled with post-welding solution heat treatment and aging. Welds made using the EBW process also exhibit high strength. Hardness measurements revealed that softening occurred within the HAZ. A variety of welding processes have been used with Weldalite and the magnitude of the softened region has been shown to be dependent on the heat input associated with the welding processes employed. Mechanical tests also revealed the tendency of increased weldment strength and toughness at cryogenic temperatures in this alloy.[50]

Resistance welding can also be used to join Al–Li–X alloys. Since the resistivity of these alloys increases with lithium concentration (Fig. 12), the applied welding current[51] required is lower than for other aluminium alloys. Ryazantsev *et al.*[52] report that successful

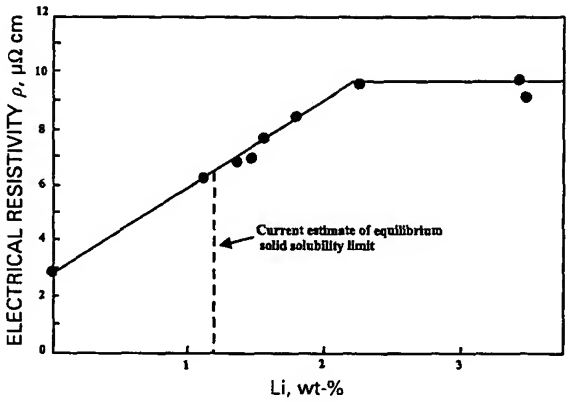

12 Electrical resistivity of mechanically alloyed Al–Li binary systems increases with lithium content beyond equilibrium solid solubility limit[4]

resistance spot welding was performed on alloy 01420 and the welding force required was lower than that for other high strength aluminium alloys. Gittos[51] reports that resistance spot and seam welding of alloy 8090 were also easily accomplished. However, spot welds were found to exhibit inferior mechanical properties since they cracked easily along the fusion boundary. Although not reported by Gittos, this phenomenon may result from the formation of a crack susceptible equiaxed grain zone along the fusion boundary, as is discussed in a subsequent section.

Friction stir welding (FSW) of Al–Li–X alloys has been investigated as an alternative to arc welding,

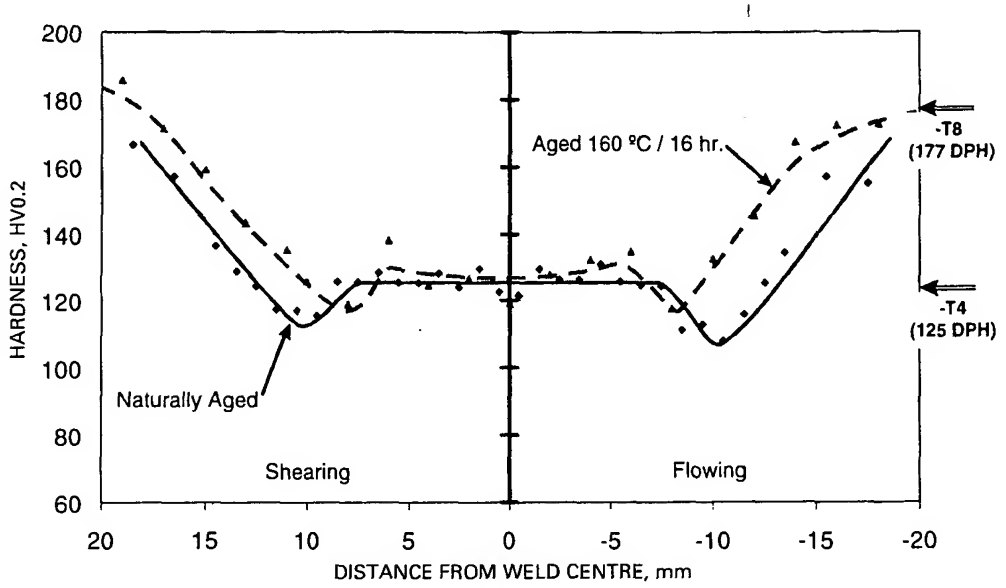

13 Hardness profile across friction stir weld in alloy 2195 in as welded condition and after natural aging[54]

since it is a solid state process that has the potential for improving mechanical properties and avoiding defects such as porosity and weld solidification cracking. The process uses a non-consumable tool which spins along the joint line and 'stirs' the material at elevated temperature to create a weld.[53] Work by Ditzel[54] and others on alloy 2195 has shown that the stir zone (SZ), where extensive plastic deformation takes place, consisted of very fine grains. This is attributable to dynamic recrystallisation which occurs within this region. Friction stir welding has been proven capable of developing good tensile properties with efficiencies approaching 75% in post-weld artificially aged condition (PWHT at 160°C for 8 h).

Post-weld natural aging also results in significant hardness recovery, indicating that the precipitates in the SZ were put into solution during welding, allowing for subsequent re-precipitation by either artificial or natural aging (Fig. 13). The absence of any melting in the SZ keeps solute in solid solution eliminating eutectic formation at grain boundaries, thereby improving the natural aging response relative to fusion welds. The response to post-weld aging treatments in zones like the heat and deformation affected zone (HDAZ) located next to the SZ or the true HAZ was similar to that of the SZ though the HAZ exhibited a pronounced minimum in hardness. However, softening in the HAZ was not shown to be the property limiting region in alloy 2195. Rather, failures were associated with either incomplete bonding at the root of the weld or pore formation at the top of the weld. In the absence of these process related defects, it is likely that the joint efficiency of the friction stir welds would be superior to that of comparable fusion welds.

Weld cracking susceptibility

Weld metal solidification cracking

Weld solidification cracking is an inherent problem in many structural aluminium alloys resulting from a combination of a large solidification temperature range and significant contraction stresses that arise due to a large coefficient of thermal expansion. The interrelationship among alloy composition, solidification temperature range, and the amount and nature of eutectic constituent that forms during the final stages of solidification controls cracking susceptibility in aluminium alloys. Weld solidification cracking usually occurs along solidification grain boundaries. Partitioning of alloy and impurity elements during solidification promotes the formation of low melting liquid films along these boundaries which may separate, i.e. crack, if sufficient stress is imparted across the boundary.[55] The effect of composition on weld metal cracking susceptibility can be explained using the simple eutectic phase diagram in Fig. 14.

At low solute contents the solidification temperature range is small and only a small amount of eutectic forms during the final stages of solidification resulting in a crack resistant structure. As the solute content approaches the solid solubility limit both solidification temperature range and amount of eutectic liquid at grain boundaries increase. High cracking susceptibility results from this combined effect. Under non-equilibrium conditions, such as during welding, this maximum response occurs at compositions below the maximum solid solubility.[56,57] As the solute content increases above the maximum solid solubility, the solidification temperature range again narrows and more liquid of eutectic composition is present during the final stages of solidification. The increased eutectic product will tend to 'heal' any cracks which form. Thus, cracking resistance in aluminium alloys can generally be achieved with either 'solute lean' or 'solute rich' compositions.

This is illustrated in Fig. 15 for the Al–Cu, Al–Li, Al–Mg, and Al–Si systems based on solidification cracking data generated using these binary systems.[57,58] Rather than the actual composition, a value normalised by the maximum solid solubility is used so that all the alloys can be plotted relative to the

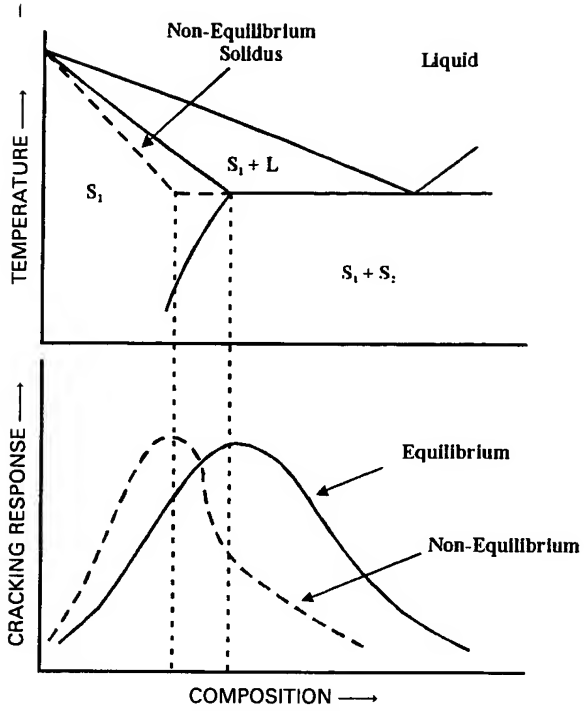

14 Weld metal cracking susceptibility as function of composition in simple binary alloy system containing a eutectic reaction: both equilibrium and non-equilibrium solidification conditions considered

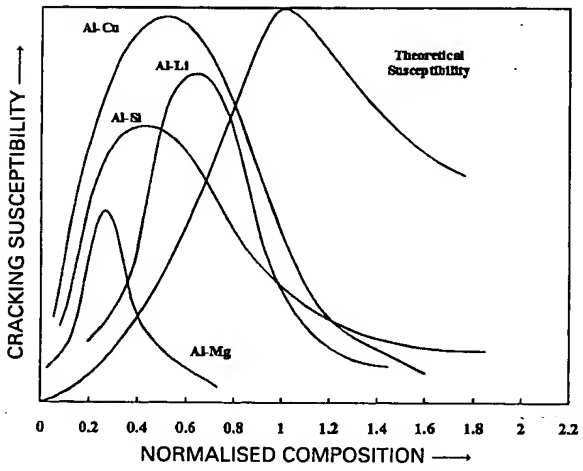

15 Cracking susceptibility *v.* normalised composition (C_0/C_{max}) for Al–Cu, Al–Mg, Al–Li, and Al–Si binary systems

theoretical peak in cracking susceptibility under equilibrium conditions (Fig. 14).

Based on the curves in Figs. 15, 16, and 17 the peak in cracking susceptibility occurs at 2·5%Li, 3%Cu, 3%Mg, and 0·8%Si. Note that these concentrations are very close to the nominal composition of many of the commercial alloys listed in Table 2. Thus, it is not surprising that many of the Al–Li–X alloys show some level of susceptibility to weld solidification cracking. It should be noted that most Al–Li–X base metals were designed to optimise strength and the

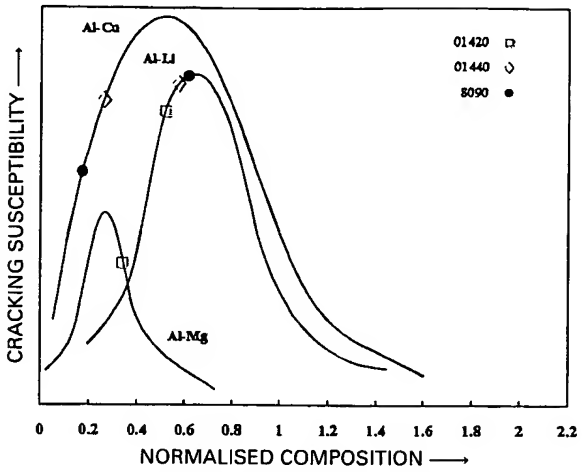

16 Cracking susceptibility *v.* normalised composition (C_0/C_{max}) for Al–Cu, Al–Mg, and Al–Li binary systems; location of various alloys shown

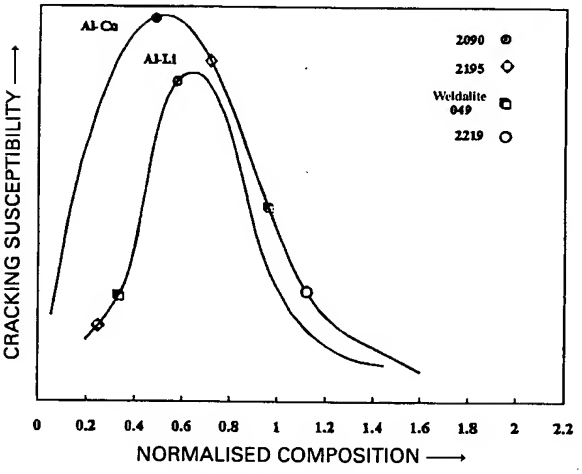

17 Cracking susceptibility *v.* normalised composition (C_0/C_{max}) for Al–Cu and Al–Li binary systems; location of various alloys shown

compositions that promote good mechanical properties may not be optimum for weld cracking resistance.

The information from Fig. 15 can further be used to estimate the weld solidification temperature range and fraction eutectic that results in a maximum in cracking susceptibility. This is done by taking the composition at the point of maximum cracking susceptibility in Fig. 15 and determining the temperature differential between the liquidus at this composition and the eutectic temperature, using the appropriate

Table 4 Solidification temperature range and fraction eutectic at maximum cracking

Alloy system	Composition of maximum cracking, wt-%	Solidification temperature range, K	Fraction eutectic, vol.-%
Al–Li	2·5	55	9·9
Al–Cu	3·0	100	5·5
Al–Mg	3·0	205	1·4
Al–Si	0·8	90	4·2

binary phase diagram. The Scheil equation[59] is used to estimate the fraction of eutectic liquid for the composition of maximum cracking, again based on the binary phase diagrams. This data is provided in Table 4.

Estimates of solidification temperature range and fraction eutectic can also be determined for the commercial alloys using binary systems. These data are provided in Table 5. It is recognised that these serve only as estimates, since there will be interactive effects among elements. Unfortunately, ternary systems are not available for Al–Li–X alloys to make these estimates more accurate.

The data in Tables 4 and 5, and Figs. 15–17 can be used to provide some estimate of weld solidification cracking susceptibility by comparing the solidification temperature ranges and determining how close the nominal composition is to the peak in cracking susceptibility in Table 4. For the Al–Cu–Li alloys, the addition of Cu appears to expand the solidification range in all cases. Alloys such as 2090 and 2091, whose Cu and Li content are very close to the Cu and Li peaks in Fig. 17 (3·0 and 2·5 wt-%, respectively) would be expected to be very susceptible to cracking. In contrast, an Al–Cu alloy such as 2219, which has a Cu content of 6·5 wt-%, is relatively resistant to weld solidification cracking. This results from both the narrowing of the weld solidification temperature range and the large amount of eutectic that forms at the end of solidification.

The fraction eutectic can also serve as a good measure of cracking susceptibility. From Table 4, it can be seen that cracking is a maximum in the binary systems when the amount of eutectic is between 4 and 10% (ignoring the Al–Mg system). At levels below this, insufficient liquid of eutectic composition is present at the end of solidification to completely wet the grain boundaries. At higher levels, sufficient liquid is present to heal cracks that may form. This explains the characteristic of eutectic systems, whereby cracking susceptibility first increases to a maximum and then decreases with the addition of solute. For the Al–Cu–Li system, the reduction of Li below 2·5% and increase in Cu above 3·0% should reduce cracking susceptibility. This was the approach taken with the development of the Weldalite family of alloys in order to improve their weldability.[56,60] The negative effect of Cu on cryogenic fracture toughness, however, resulted in the reduction of Cu levels in these alloys to around 4·0%.

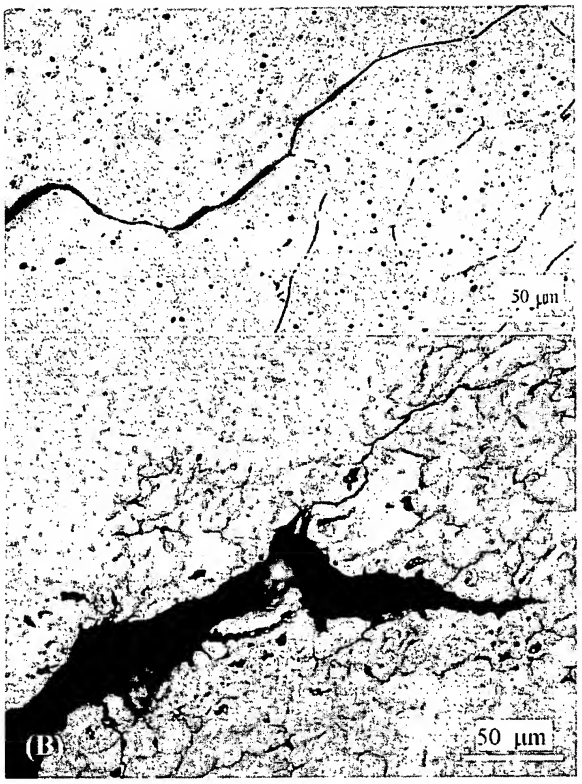

A alloy 8090; *B* alloy 2195; arrow *B* highlights tip of crack

18 Representative weld solidification cracking in Varestraint samples tested at 3% strain

In spite of its large solidification temperature range (Table 5), alloy 01420 is reported[2,4,5] to show good weldability. From Fig. 15 and Table 4 it can be seen that the binary Al–Mg system has a peak in cracking susceptibility at ~3·0 wt-%Mg.[16] The high Mg content of this alloy (5·3 wt-%) places alloy 01420 away from the cracking susceptible regime.

Figure 18 shows representative weld metal solidification cracks in autogenous welds in alloys 8090 and 2195. This cracking was produced using the Varestraint test as described below. As is typical, weld solidification cracks follow solidification grain boundaries since these are the last regions to solidify. Note that these boundaries exhibit a continuous network of eutectic constituent. This indicates that liquid films of eutectic composition existed along these boundaries at the end of solidification. There is no evidence of

Table 5 Solidification data for commercial Al–Li–X alloys based on binary phase diagrams

	Predicted weld solidification temperature range, K			Fraction eutectic calculated from Scheil equation (Ref. 59)		
Alloy	Al–Li	Al–Cu	Al–Mg	Al–Li	Al–Cu	Al–Mg
01420	48	...	178	6·8	...	3·6
8090	45	109	...	9·9	1·5	...
2020	53	97	...	2·9	8·8	...
2090	46	103	...	8·6	4·9	...
2091	48	105	...	6·8	3·8	...
2094	52	96	...	3·3	9·6	...
2095	54	98	...	2·2	7·9	...
2195	54	98	...	2·2	7·9	...
2014	...	97	...	...	9·1	...
2219	...	91	...	...	13·6	...

'backfilling' in either of these alloys, suggesting that the amount of liquid was sufficient to wet the boundary, but insufficient to heal any cracks that might form. This is consistent with the data in Table 5 that suggests fraction eutectic of the order of 5 vol.-%.

Weld solidification cracking susceptibility data from the literature have been generated using different types of test such as the Varestraint and Houldcroft tests. Since these tests are fundamentally different and neither is standardised, it is difficult to compare results published by different investigators. Recently, Lippold and Lin[55] have proposed a technique using the Varestraint test that measures the actual solidification cracking temperature range (SCTR) in the fusion zone. This is an alloy-specific parameter determined by measuring the length of the longest solidification crack in a test sample where the cooling rate and solidification velocity are known. Data gathered for various Al–Cu and Al–Cu–Li alloys are presented in Table 6. Note that the SCTR is greater than the predicted solidification temperature range shown in Table 5 for both the Al–Cu and Al–Li systems. This suggests that the interactive effects of Cu and Li in conjunction with other alloying elements or impurities (Mg, Si, Mn, Fe, etc.) tend to extend the solidification temperature range to lower temperatures.

Increased resistance to weld solidification cracking has been reported in both Weldalite 049 and 2090 alloys in studies using filler metals[56] with high copper content, such as 2319. Figure 7 shows the weld metal microstructure of the alloy 2195 welded using 2319 filler metal. The effect the higher volume fraction eutectic in this structure relative to lower Cu alloys (Fig. 6) is apparent.

Additions of Mg result in lower melting point Mg-rich eutectics which extend the 'mushy' solidification range and change the wetting characteristics of the interdendritic liquid, thus promoting solidification cracking.[56] Small amounts of Ti refine solidification grain sizes and thus the distribution of eutectic liquid at grain boundaries is modified resulting in lower cracking susceptibility. High levels of Ti are reported to result in the formation of brittle intermetallics at the grain boundaries thus, promoting higher cracking susceptibility in the solid state.[56]

Alloy 01420 has been reported to exhibit 'good weldability'[2,4,5] when using filler materials boosted in Mg and with small Ti additions. Low copper, high magnesium 8090 alloys have also been reported[3,5,61] to exhibit good resistance to cracking when using Al–Mg based (5000 series) filler materials.

Table 6 Maximum crack distance (MCD) and solidification cracking temperature range (SCTR) determined using Varestraint test[55]

	Longitudinal Varestraint		Transverse Varestraint	
Alloy	MCD, mm	SCTR, K	MCD, mm	SCTR, K
2014	6·3	185	...	...
2219	3·9	155	2·04	125
2090	7·2	190	...	...
2094	14·5*	225	...	...
2195	13·3*	220	4·07	182

*Contribution from fusion boundary cracking.

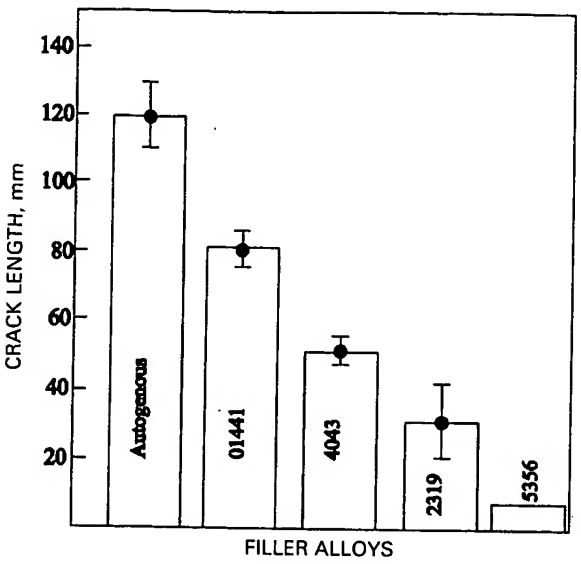

19 Cracking susceptibility of autogenous and filler metal welds on 01441–T8 aluminium alloy sheets[17] using Houldcroft test

Employing the Houldcroft test, Reddy *et al.*[17] conducted weldability studies for the alloy 01441 using a range of filler alloys, namely, 01441, 4043, 2319, and 5356. It was found that weld cracking susceptibility was reduced in the order: autogenous, 01441, 4043, 2319, 5356 (Fig. 19). Alloys 4043 and 2319 have the smallest solidification temperature range (61 K and 46 K, respectively), which is significantly lower than that for the alloy 01441 (106 K). It is also known that fillers 4043, 2319, and 5356 are eutectiferous alloys. The fact that alloy 5356 results in better overall weldability irrespective of its higher solidification temperature range, is attributed to the fact that the eutectic liquid is not continuously distributed around the grain boundaries thus allowing an extensive network of solid–solid bridges to form during the last stages of solidification.

The weldability of some commercial Al–Li–X alloys that contain Cu and Mg can be assessed using a map of total crack length (TCL) versus Cu and Mg content,[62] as shown in Fig. 20. This map does not reflect the influence of Li, but shows how the combined effects of Mg and Cu influence cracking susceptibility. It is interesting to note that the peak in cracking susceptibility is very close to the 1·4%Mg and 3·0%Cu values from Table 4 for maximum cracking in binary systems. High levels of either element reduce susceptibility, as shown in alloys 2219 or 5083. Alloys containing substantial amounts of both elements such as 2024 (4·4Cu, 1·5Mg) and 7075 (1·6Cu, 2·5Mg) are known to have poor weldability as reflected by their high values of TCL. Based on Fig. 20, the order of increasing resistance to cracking of some of Al–Li–X alloys is 2091, 8090, 2090, and Weldalite 049.

HAZ liquation cracking

Heat affected zone liquation cracking by definition is a type of high temperature weld cracking which takes place in the HAZ adjacent to the fusion boundary and is associated with the formation of liquid films

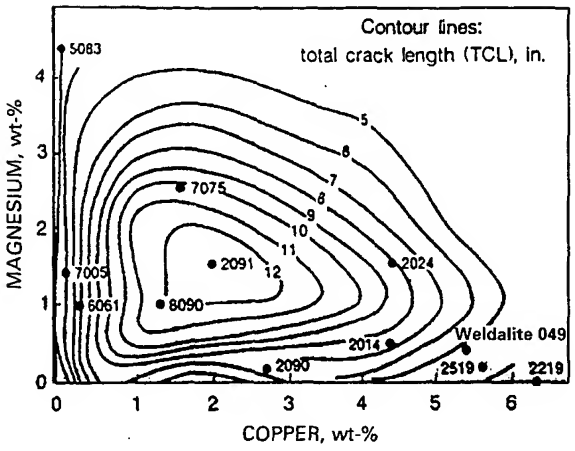

20 Total crack length contour map: Li-bearing aluminium alloys 8090, 2090, 2091, and Weldalite 049 are superimposed[62,63]

at grain boundaries. This region is defined as the partially melted zone (PMZ) of the HAZ. Although metallurgically this type of cracking is associated with the presence of liquid, no theories exist that quantify the potential for HAZ liquation cracking based only on the amount and/or the characteristics of the liquid evolved. Sufficient tensile stress is also required in order for cracking to occur (crack initiation) and such stresses do not generally develop until the weld pool begins to cool.

Since the PMZ is a region adjacent to the fusion zone where melting ranges from 0 to 100%, evolution of liquid in the HAZ is, by definition, confined to the PMZ. The peak temperatures experienced by PMZ fall between the liquidus T_L and effective solidus of the BM. The effective solidus is always below the equilibrium solidus due to segregation, which is invariably present in commercial aluminium alloys.[64]

In general, the paucity of data currently available in the literature precludes a straightforward assessment of HAZ liquation cracking in Al–Li–X alloys. In addition, those data have been generated using a variety of tests such as the Gleeble hot ductility test or the Varestraint test. Results from different types of test cannot be directly compared since each test uses different criteria in assessing weldability.

Using the Gleeble hot ductility test Zacharia *et al.*[65] studied the HAZ liquation cracking of alloys 2090 and 2091. They concluded that both alloys do not exhibit a strong tendency for HAZ liquation cracking, since the temperature range in which the material recovers its ductility on cooling from the peak HAZ temperature is extremely small. The same conclusions were drawn by Yunjia *et al.*,[66] who studied the weldability of both 2090 and 2024 alloys using the Varestraint test. Alloy 2090 was judged to be less susceptible to HAZ liquation cracking compared with alloy 2024. In another study Yunjia *et al.*[67] studied the weldability of both 8090 and 2024 alloys using the transverse Varestraint test. They again concluded that alloy 8090 was less prone to HAZ liquation cracking compared with the 2024 alloy.

Studies were performed by Ilyushenko *et al.*[43] to simulate the response of the HAZ of alloy 01420 at different thermal cycles using isothermal soaking of specimens in a molten tin bath. Specimens previously had been heated to different temperatures. It was deduced that by heating in the range 550–580°C ($T_L = 635$°C for 01420 alloy) both dissolution of the strengthening phases and extensive melting of primary intermetallic compounds took place. Hardness of those specimens was measured to be minimal and it could not be restored even after artificial aging (at 160°C for 16 h). Although the tendency of liquid formation was traced in the previous work, strain and/or strain rate effects were not examined. Consequently, the overall HAZ liquation cracking susceptibility of alloy 01420 was not clearly determined.

The weldability of several variants of Weldalite 049 alloy with different levels of Cu content was studied by Kramer *et al.*[60] using the spot Varestraint test. Alloys 2090, 2219, and 2014 were also examined. Employing the total crack length (TCL) in the HAZ as a weldability criterion, it was shown that little or no cracking occurred in the HAZ of alloys 2090 and Weldalite 049. However, a significant amount of HAZ cracking was found in alloys 2219 and 2014 (*see* Table 7). Liquation of low melting point eutectics on grain boundaries accounted for the formation of cracks in the HAZ of those alloys.

It should be pointed out that the HAZ liquation cracking susceptibility of Al–Li–X alloys is also influenced by the cracking susceptibility of the fusion zone. If weld solidification cracking susceptibility is high, then cracking will tend to be concentrated in the fusion zone even if the HAZ is susceptible. In cases where filler metals are used to improve weld solidification cracking resistance (such as when 2319 is used with 2000 series alloys), it is possible that HAZ liquation cracking could be a problem in some alloys. It is understood that when the weld cracking resistance of the weld metal is improved by filler metal selection, the susceptibility of the HAZ may then be realised since liquated HAZ grain boundaries may then become the weakest link in the microstructure.

Equiaxed grain zone formation and associated fusion boundary cracking

An equiaxed grain zone (EQZ) along the fusion boundary, not present in other aluminium alloys, has been observed in Al–Li–X alloys.[66,68–70] This region consists of fine equiaxed grains and is located adjacent to the fusion boundary within the fusion zone. The grain boundaries are typically decorated with a eutectic constituent.[68] Careful microscopic examination of

Table 7 Spot Varestraint test results[60]

Alloy	TCL* per sample	
	Average	Standard deviation
Weldalite 049 variants		
6·1Cu	0·0	0·0
5·2Cu	0·5	0·9
4·8Cu	0·0	0·0
2090	0·0	0·0
2219	8·2	0·7
2014	9·0	2·8

* Total crack length in weld heat affected zone.

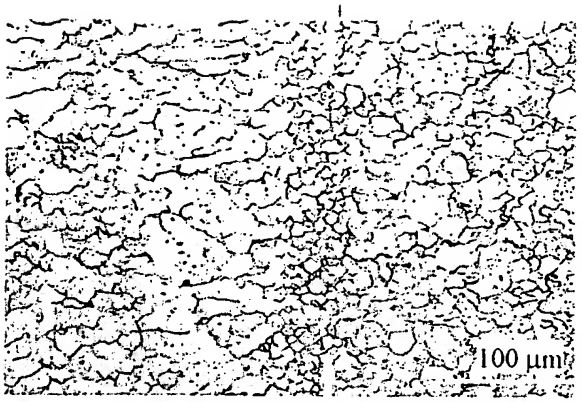

21 Fusion boundary region in Varestraint sample of alloy 2195; arrows indicate location of fusion boundary, fusion zone is on left

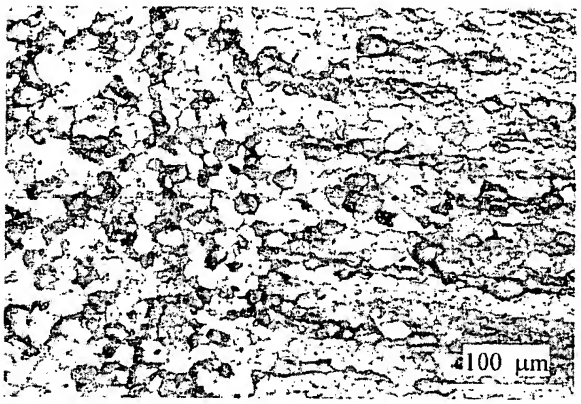

22 Fusion boundary region in weld of alloy 2195 using 2319 filler metal; arrows indicate location of fusion boundary, fusion zone is on right

the EQZ has revealed[68,69] that the fine grains do not have dendritic morphology (Figs. 21 and 22). Not all Al–Li–X alloys exhibit an EQZ, as shown in the photomicrograph of the fusion boundary of alloy 8090 (Fig. 23).

The EQZ has been associated with severe cracking during fabrication and repair of structures. This cracking has been reproduced in Al–Li–X alloys using the Varestraint test. Cracking is most often not isolated in the EQZ, but may propagate from the HAZ and/or weld metal to the fusion boundary and continue along the EQZ.[68,69] Studies by Lippold and Lin[55] have shown that vigorous stirring of the weld pool eliminates the EQZ and prevents this form of cracking.

Currently two theories have been proposed to explain EQZ formation.[66,68,69] The first hypothesis[68] is based on the premise that the EQZ is located in the PMZ and forms by a recrystallisation mechanism. It is proposed that during the weld thermal cycle the HAZ immediately adjacent to the fusion boundary undergoes recrystallisation and grain boundary liquation within the PMZ/HAZ. The second hypothesis proposed by Gutierrez *et al.*[69] and Yunjia *et al.*[66] involves a solidification mechanism requiring both nucleation and growth. It is based on heterogeneous nucleation within a molten layer near the fusion boundary, perhaps a stagnant liquid region defined

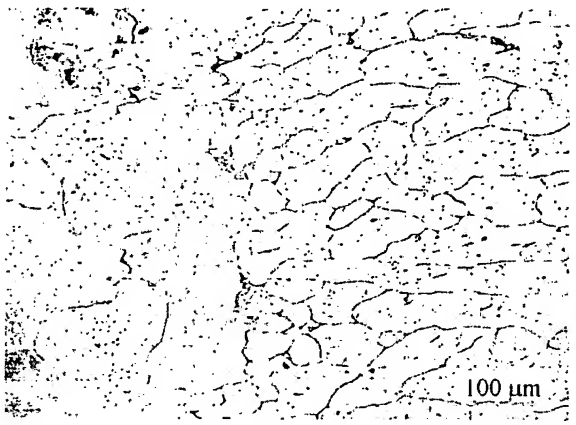

23 Fusion boundary region in Varestraint sample of alloy 8090; arrows indicate location of fusion boundary, fusion zone is on right

by the unmixed zone. Solid nuclei (precipitates or dispersoids) that are able to survive the thermal conditions (Fig. 24) in this region serve as heterogeneous nucleation sites for growth of the equiaxed grains. Yunjia *et al.* proposed that dispersoids such as Al_3Ti, Al_3Zr, or $Al_3(Li_x,Zr_{1-x})$ are possible nuclei. Such nucleating particles exist in the parent metals following homogenisation and solution heat treatment operations.[69,70]

Guttierez *et al.* and Lippold *et al.* showed that the EQZ can be eliminated by altering one of the following: (1) weld pool stirring, (2) composition, and (3) nature of the base metal. As noted above, vigorous weld pool fluid flow can effectively stir the EQZ away. In a simple laboratory experiment, an electromagnetic coil around a gas tungsten arc torch was used to rapidly spin the molten pool during welding. Fusion zones produced in this fashion exhibited no EQZ, while those produced under similar conditions but without the coil showed a distinct EQZ. Guttierrez *et al.* also clearly showed the effect of composition on EQZ formation. In special alloys made with varying Li and Zr, alloys with less than 0·5%Li and 0·04%Zr did not exhibit an EQZ. Unfortunately, the individual (uncoupled) effects of Li and Zr could not be studied.

In a study of weld substrate effects, it was found that no EQZ formed when the substrate was as welded (or cast). This occurs because the nucleating particles are dissolved or melted, and do not reform during weld cooling. When these welds are solutionised and then rewelded, the EQZ reappears, presumably because the nucleating particles have reformed during the solution heat treatment.

All the recent evidence and experimentation with respect to EQZ formation supports the nucleation and growth hypothesis proposed by Guttierrez and Lippold,[70] and Yunjia *et al.*[66] Both the stirring experiment and the effect of changing base metal substrate refute a recrystallisation hypothesis as a means for producing equiaxed grains along the fusion boundary.

Most recently, Kostrivas and Lippold[71] have studied the thermal and metallurgical conditions necessary to promote EQZ formation by performing carefully controlled melting experiments. Using the Gleeble,

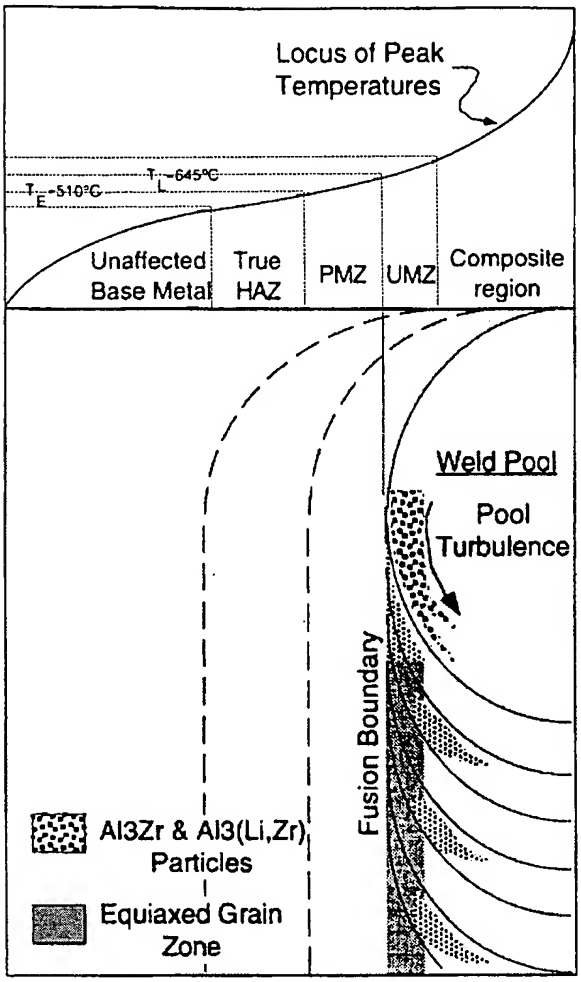

24 Schematic illustration of suggested heterogeneous nucleation mechanism for formation of equiaxed grain zone[70]

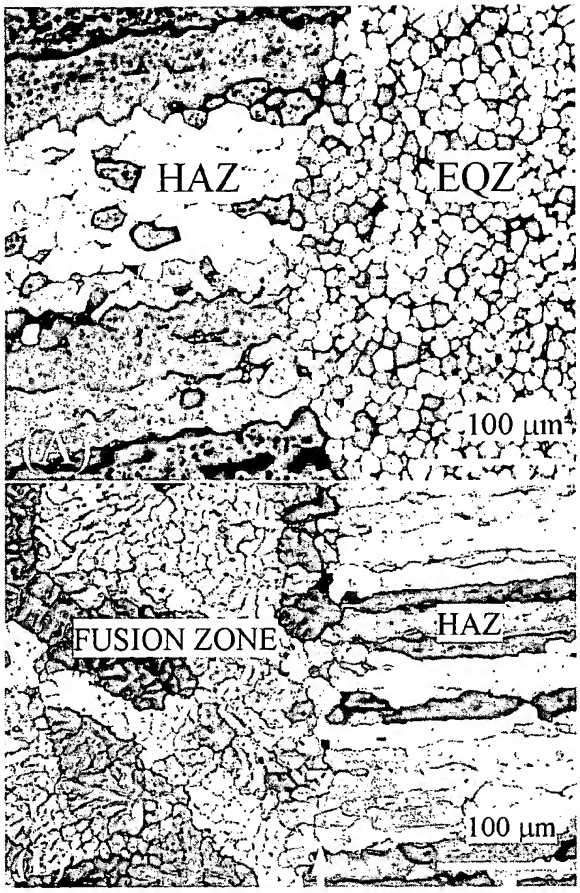

A 630°C; *B* 660°C

25 Simulated fusion boundary region in alloy 2195 produced using Gleeble

samples are heated to various temperatures above the liquidus temperature, held for a few seconds, and then cooled. For alloy 2195, an EQZ forms approximately in the temperature range 630–645°C. When similar samples are heated above 650°C the EQZ disappears and a dendritic structure is observed, as shown in Fig. 25. Again, this clearly supports the mechanism shown in Fig. 24 whereby nucleating particles that are stable in a narrow temperature field adjacent to the fusion boundary are able to promote EQZ formation. Further from the fusion boundary within the fusion zone, these particles dissolve and normal dendritic growth occurs.

Weld porosity formation and prevention

Lithium bearing aluminium alloys have been found to be particularly susceptible to porosity during welding, unless special precautions are taken. A number of studies have been performed to define the source of porosity and how to control it. Many of the studies concentrated on the Russian[2,4] alloy 01420, but other Al–Li–X alloys also exhibit porosity problems. High hydrogen and lithium concentration was observed in the surface oxide of alloy 01420, and to a significant depth below the surface (Fig. 26) as determined by secondary ion mass spectroscopy (SIMS).[47] Polished sections revealed considerably lower concentrations of hydrogen.

It is known that aluminium oxide is hydroscopic and promotes absorption of ambient moisture. The porosity in weld metals arises due to supersaturation of hydrogen in the fusion zone and subsequent formation of hydrogen bubbles during solidification.[2] Because of this tendency for moisture absorption and the large difference in hydrogen solubility between liquid and solid, porosity is a common problem when welding aluminium alloys. It has been proposed[2,4] that lithium containing compounds such as LiO_2, LiOH, $LiCO_3$, and Li_3N form in the surface layer of Al–Li–X alloys and increase the level of moisture absorption relative to other aluminium alloys. It is also reported[4] in the literature that LiH compound formation takes place at temperatures above 420°C.

A number of methods have been evaluated in an effort to reduce weld fusion zone porosity. The most effective methods include chemical and/or mechanical milling. In this case removal of at least 0·13 mm surface layer from each side of the specimen (for full penetration welds) before welding reduces porosity significantly.[2,4,5,51,59] Chemical milling has the advan-

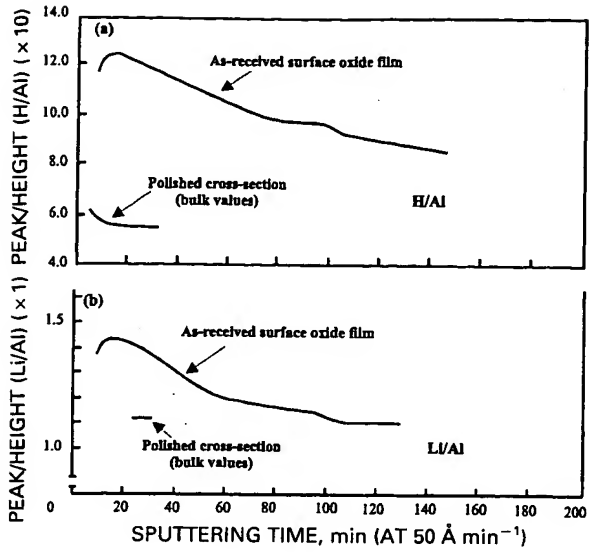

26 SIMS surface analysis of alloy 01420 (Ref. 47)

tage that it can be performed on a wide variety of shapes where mechanical milling may be difficult. When thinner sheets are to be welded, more surface material should be removed to ensure low level porosity in the weldment[72] since the surface will constitute a higher percentage of the material in the weld fusion zone. The effects on weld metal porosity of both surface preparation and time elapsed between surface machining and welding are given in Table 8 for alloy 8090. Welding immediately following surface preparation results in reduced porosity since moisture absorption from the air is minimised.[73]

Vacuum heat treatment before welding was found to help in reducing weld metal porosity by driving off hydrogen. Vacuum heat treatment was performed[4,74] on 01420 alloy specimens for 12–24 h and in the temperature range 450–500°C. This technique was also used for experimental ingot metallurgy and powder metallurgy Al–Li–X alloys which were vacuum heat treated for 12–60 h in the temperature range 482–565°C. Weldments produced subsequently were found to have low levels of porosity. It should be recognised that these thermal treatments will result in softening of the base metal. As a result, aging following welding will be required to recover mechanical properties. In addition, this method cannot be used for large structural components and is economically restrictive.

Table 8 Effect of surface preparation on weld metal porosity in alloy 8090-T6 (Ref. 73)

Surface preparation	Porosity, % weld metal area
As received, unmachined	11·0
Machined ~96 h before welding	1·8
Machined ~48 h before welding	0·8
As received, chemically pickled	1·3
Machined, solution treated, welded 20 h after solution treatment	6·0
As above, but weld immediately after solution treatment	0·5

During welding, proper torch shielding and inert backing gas is normally recommended to maintain porosity at acceptable low levels. Electron beam welding was found to be very effective in reducing the incidence of porosity.[4,5] Finally laser beam welding (LBW) produced welds with low porosity[75] and has the advantage of allowing welding of large sections under ambient conditions without filler material, enabling precise control of the amount of heat imparted on the workpiece.[76]

Corrosion behaviour

An important aspect of the industrial application of Li-bearing aluminium alloys is their corrosion behaviour. Specifically, the resistance to stress corrosion cracking (SCC) is an important criterion in the selection of high strength aluminium alloys for aerospace applications.[2] Welding can have a significant influence on corrosion resistance due to the change in microstructure that occurs and the presence of residual stresses. In aluminium alloys, SCC and pitting are the forms of corrosion that most often affect structural integrity. To date, relatively few papers have addressed the corrosion behaviour of weldments. The following paragraphs summarise observations related to base metals.

A number of papers have been published[77–85] which deal with SCC and pitting corrosion resistance of Al–Li–X base materials in saline solutions or salt fog environments. It is expected that these observations will apply to welded structures. In general, Al–Li–X alloys are not immune to corrosion but their susceptibility is at least equal, if not lower, than conventional high strength aluminium alloys.[9,79] Lack of uniformity in distribution of anodic phases like δ-AlLi, T_2-Al_6CuLi_3, etc., along grain boundaries, is considered responsible for intergranular attack, since anodic phases will pit and corrode in the presence of an electrolyte to protect cathodic metal and, as a result sharp propagating fissures can potentially form.[5,78,79]

Kumai *et al.*[32] have studied the pitting corrosion as a function of aging at 200°C of an Al–Li and an Al–Cu–Li (2090) alloy both in chloride ion media and in solutions free of chloride ions. Central to their findings is a precipitation free zone (PFZ) in both the Al–Li and Al–Cu–Li alloy.

On aging of the Al–Li alloy, precipitation of δ' phase took place throughout the microstructure. Absence of δ' precipitates was observed only in regions (PFZ) immediately adjacent to solidification grain boundaries (Fig. 27). However, preferential grain boundary and subgrain boundary corrosion did not take place in either the solution heat treated (SHT) or aged condition. Therefore, it is concluded that lithium did not adversely affect the pitting of the binary Al–Li alloy. In the Al–Cu–Li alloy, SHT and aging results in precipitation of Cu-rich phases like Θ' or T_1, on both solidification grain boundary and subgrain solidification grain boundary and in the formation of zones that are free of Cu-rich precipitates and depleted in copper (Fig. 27). It is suggested that these Cu depleted zones are responsible for both intergranular cracking (IGC) and intergranular stress corrosion cracking (IGSCC).[32] It is interesting to

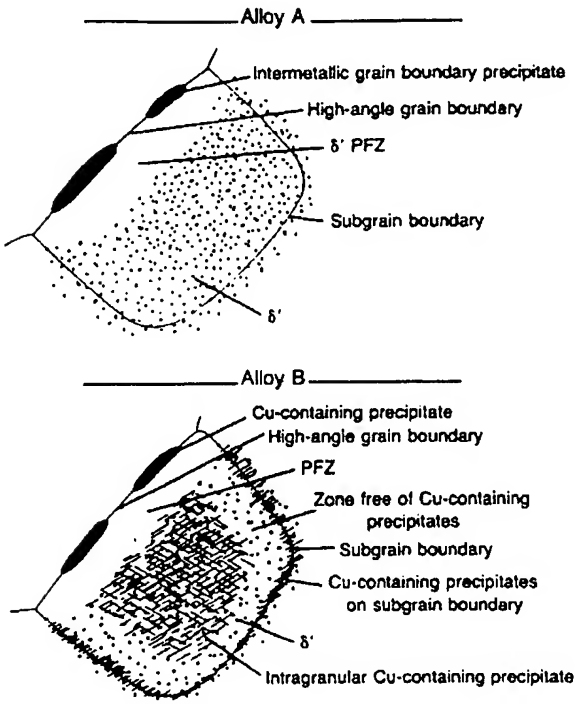

27 Schematic illustration of phase changes occurring and resulting PFZs within alloys *A* and *B* as result of solution heat treatment and aging at 200°C; alloy *A* is an Al–Li–Zr system while alloy *B* is an Al–Cu–Li–Zr base system[32]

note the absence of grain boundary corrosion in samples that were stretched (cold worked) before aging.[32] Stretching results in homogeneous precipitation during subsequent aging and the absence of Cu depleted zones.

Other studies[82,83] point out the role of hydrogen on corrosion. A brittle hydride having the composition $LiAlH_4$ forms in Al–Li–X alloys under conditions of severe SCC. This mechanism of cracking requires hydrogen generation, hydrogen diffusion into the material and hydrogen concentration in a localised region of the material that would cause hydrogen embrittlement. It is suggested that hydrogen is generated on the surface by the reduction of hydrogen ions while hydrogen entry into the material is made easy by breaking down the protective oxide film on the surface. Diffusion assisted by dislocations and grain boundaries drives hydrogen into the material and on hydrogen saturation the brittle $LiAlH_4$ hydride forms from the solid solution or from Li-bearing precipitates, e.g. δ' or δ. Repeated formation and cleavage of the hydride ahead of the advancing crack tip thus promotes SCC. Some observations of SCC in Al–Li alloys and their explanation are given in Table 9.

Some corrosion studies[83] reveal the detrimental effect of the atmospheric CO_2 when the Al–Li–X sample is removed from the saline environment. During immersion, samples were found to pit but did not fail by SCC.[72] It is reported that aggressive corrosion of the α-Al subgrain boundary fissure walls occurs when the specimen remains immersed in the chlorine environment and this prevents a sharp crack from forming. Instead blunt non-propagating fissures are produced. On removing the specimen from the bulk solution, the dissolved CO_2 seems to help passivation of subgrain boundary fissure walls by formation of $Li_2[Al_2(OH)_6]_2.CO_3.3H_2O$, which causes the crevice potential to increase. Under these conditions vigorous dissolution of T_1 phase takes place while the crack walls remain passive. As a result the sharp crack formed propagates rapidly along an active path defined by SGB containing large T_1 phase and Cu depleted zones under the influence of electrochemical action and applied stress. When a critical flaw size is achieved overload fracture occurs.

Martukanitz *et al.*[72] have shown that both electron beam and gas metal arc (GMA) welds in alloy 2090 using both 2319 and 4043 filler metal exhibit good resistance to SCC. Corrosion potential is relatively low at the fusion boundary, where stresses are the highest, indicating that this region is protected by the anodic base metal (Fig. 28). Weldments of the alloy 01420 produced by both EBW and argon arc welding processes (gas tungsten arc welding (GTAW)) have also been reported to exhibit good SCC behaviour.[4]

Summary

Lithium bearing aluminium alloys can be welded using a variety of processes including gas tungsten arc, plasma arc, laser beam, electron beam, resistance, and friction welding. The use of these alloys is not restricted to certain welding processes and process selection is equivalent to other structural aluminium alloys. A variety of standard (Li free) filler metals can be used with these alloys. Lithium bearing filler metals are not generally available, or recommended, because of increased potential for porosity formation.

Table 9 Hydrogen embrittlement in Al–Li–X alloys[82]

Observations	Proposed hydride cracking mechanism
Presence of stable hydrides indicated by tritium release characteristics, by SIMS and by laser microprobe spectroscopy	Systems that form hydrides can be embrittled by hydrides
Discontinuous crack propagation in the absence of dislocation at crack tip	Diffusion of hydrogen to the region ahead of the crack tip to form hydride and its subsequent failure
Increased faceted appearance of the fracture surface with increased hydrogen precharging	Longer precharging times leads to enhanced hydride formation and enhanced embrittlement
Hydrogen interaction with the SGB and SSGB precipitates caused embrittlement	Hydrogen interacts with the grain boundary AlLi phase to form $LaAlH_4$ and the hydride can favourably nucleate at the SSGB
Intergranular fracture mode in SCC with very little microductility	Hydrogen interacts with AlLi to form $LiAlH_4$ at SGB
Ease of crack initiation at SGB and decrease in K_{ISCC} with aging or higher Li content	Hydrides formed from grain boundary AlLi act as crack initiators. Grain boundary AlLi amount increases with aging of higher Li content
Direct imaging of a brittle hydride	Strong support for the hydride crack mechanism

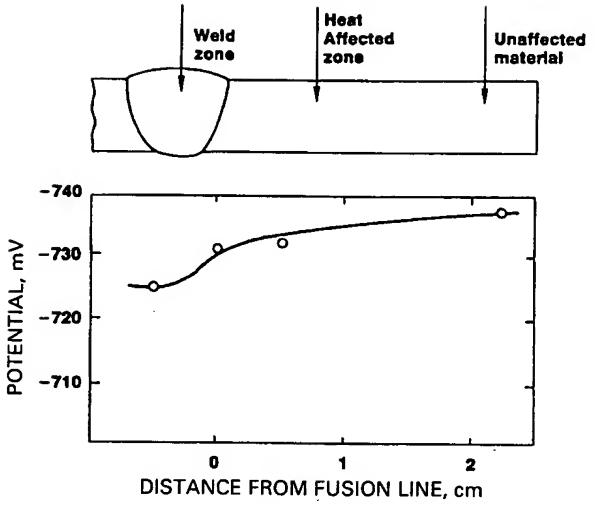

28 Potential across fusion zone and HAZ of gas metal arc weld in alloy 2090–T8 using 4043 filler metal (3·5%NaCl solution)[72]

The weldability of these alloys has been reviewed in the context of cracking during fabrication, weldment mechanical properties, weld porosity formation, and corrosion resistance. Of these issues, susceptibility to cracking and mechanical property degradation are most critical relative to the use of these alloys in welded applications. Weld porosity can be controlled if proper material preparation and cleaning procedures are employed. Limited data on the corrosion behaviour of these alloys has been published, but it appears that the addition of lithium does not adversely affect either the stress corrosion cracking or pitting corrosion resistance relative to other high strength aluminium alloys.

The low joint efficiency (ratio of weld strength to base metal strength) in Al–Li–X alloys is analogous to other high strength, precipitation hardenable aluminium alloys. Joint efficiencies for some alloys in the as welded condition may be as low as 50%. The use of non-heat treatable filler metals (such as 4043) may preclude any strength recovery via post-weld heat treatment. In any case, softening in the weld metal and heat affected zone (HAZ) can only be partially recovered by post-weld aging treatments. Solution annealing and aging following welding can improve joint efficiency dramatically, but it is usually impractical for most welded structures. Considerable research has been conducted in an attempt to optimise the weld properties of these alloys. This work has conclusively shown that achieving joint efficiencies greater than 60% is virtually impossible in alloys 8090, 2090, and 2195 unless the entire weldment is solution treated and aged. Joint efficiencies reported for the Soviet 01420 alloy are considerably better, even in the as welded condition, though the reason for this is not apparent.

Al–Cu–Li and Al–Mg–Li alloys are more susceptible to weld solidification cracking than comparable commercial alloys that do not contain lithium. By evaluating the individual effects of Li, Mg, and Cu using appropriate binary alloy systems, many of the Al–Li–X alloys were found to contain levels of alloying addition that increased cracking susceptibility. This is primarily the result of the amount and distribution of eutectic liquid in the weld microstructure, which allows grain boundaries to be wet by liquid films, but is insufficient to provide any crack 'healing' effects. Where filler metals are employed, cracking susceptibility can be reduced by the selection of appropriate filler metal compositions. In the Al–Cu–Li system, the use of filler alloys 2319, 4043, and 4047 significantly increase cracking resistance. For the Al–Mg–Li alloys, filler metals with higher Mg content than the base metal appear to improve weldability. Improvement in the inherent weld cracking susceptibility of the Li-bearing base metals will require further alloy development and consideration of the microstructural factors that control cracking susceptibility. These factors include control of the eutectic content of the weld metal through alloy additions and the use of grain refinement by the addition of elements such as titanium, zirconium, and scandium.

The presence of an equiaxed grain zone (EQZ) along the fusion boundary presents another, and more intractable, problem. Because the EQZ most likely forms from the unmixed zone region of the fusion zone, elimination of the EQZ by filler metal additions is not possible. In Al–Li–X alloys containing zirconium, the EQZ has been shown to be highly susceptible to cracking during both fabrication and repair. This aspect of weld cracking susceptibility warrants additional investigation. Recently, techniques have been developed to study EQZ formation in special samples prepared using a Gleeble thermomechanical simulator. This has proven to be a relatively efficient method to evaluate the EQZ in commercial and/or experimental Al–Li–X alloys.

Adjusting base metal compositions can influence weldability. Increasing copper content above 5 wt-% or Mg above 3 wt-% will improve weld cracking resistance by promoting more eutectic liquid healing during solidification. However, such an approach may adversely affect other material properties, such as toughness, ductility, strength, or fatigue crack resistance. 'Tweaking' of other elements may provide some improvement in weldability, for instance regarding EQZ formation, but these changes may be counter to optimising mechanical properties. Weld metal strength, though always inferior to that of the parent metal, can also be improved by implementing post-weld heat treatment and aging. But again, this is not always feasible especially for field fabrication and large scale assemblies such as cryogenic tankage.

Compositional modifications of Al–Li–X for structural applications, such as cryogenic tankage, must consider not only weldability issues such as weld solidification cracking, EQZ cracking, HAZ delamination, etc., but the implications that such modifications may have on alloy performance. Despite considerable development of Al–Li–X alloys over the past 30 years, the relationship between weld cracking susceptibility and composition is not fully understood and weldability problems persist with these alloy systems. In the absence of any systematic, coordinated study of this relationship, development of truly 'weldable' Li-bearing aluminium alloys will be difficult.

Al–Li–X alloys exhibit adequate resistance to corrosion even in chloride ion solutions. Eliminating precipitation free zones by proper mechanical treatment and aging enhances their corrosion properties. The stress corrosion threshold usually is lowest in the underaged condition where toughness is maximum and becomes lowest in the overaged condition where toughness is lowest.[86] Proper control of welding parameters and thermomechanical processing before and after welding potentially will produce optimum corrosion properties. In addition, it should be noted that zones such as the HAZ, which are difficult to restore to their original properties after welding, seem to be anodically protected by the base metal. Relative to other structural aluminium alloys, corrosion properties do not compromise the use of these alloys in engineering applications, including marine environments.

In conclusion, the Li-bearing aluminium alloys have been shown to be weldable using a variety of processes and procedures. Cracking in the weld metal and the fusion boundary EQZ still plagues many of these alloys and will require further alloy development to better control susceptibility. Further research is also warranted to better optimise weld joint efficiency through post-weld aging treatments. Improvements in the welded/aged strength of these alloys will greatly expand their engineering usefulness by offering welded aluminium structures that greatly exceed the properties of currently available structural alloys.

References

1. P. S. FIELDING and G. J. WOLF: *Adv. Mater. Process.*, Oct. 1996, **150**, (4), 21–23.
2. J. C. LIPPOLD and J. K. WATSON: 'The weldability of aluminum–lithium alloys: a review', in Proc. North American Welding Research Seminar; 1987, Columbus, OH, Edison Welding Institute.
3. C. E. CROSS and W. T. TACK: in 'Metals handbook', 10th edn, Vol. 6, 549–552; 1995, Westerville, OH, ASM.
4. J. R. PICKENS: *J. Mater. Sci.*, 1985, **20**, 4247–4258.
5. J. R. PICKENS: *J. Mater. Sci.*, 1990, **25**, (7), 3035–3047.
6. C. E. CROSS: 'Weldability of aluminum–lithium alloys: an investigation of hot tearing mechanisms', PhD thesis, Colorado School of Mines, August 1986.
7. T. S. SRIVATSAN and T. S. SUDARSHAN: *Weld. J.*, 1991, **70**, (7), 173s–185s.
8. J. T. STALEY: *Light Met. Age*, 1990, **48**, (11), 31–32.
9. S. J. CIESLAK, R. M. HART, P. L. MEHR, and L. N. MUELLER: 'Alcoa alithalite alloy 2090 technical information', paper presented at 17th Int. SAMPE Conf., Kiamesha Lake, NY, 22–24 October 1985, Society for the Advancement of Material and Process Engineering, Covina, CA.
10. J. R. PICKENS, L. S. KRAMER, T. J. LANGAN, and F. H. HEUBAUM: in Proc. 6th Int. Aluminum–Lithium Conf., Garmisch-Partenkirchen, Germany, (ed. M. Peters and P.-J. Winkler), Vol. 1, 357–362; 1991, Oberursel, DGM Informationsgesellschaft.
11. I. N. FRIDLYANDER, A. G. BRATUKHIN, and V. G. DAVYDOV: *Russ. Metall.*, 1992, (3), 107–109.
12. A. G. BRATUKHIN: *Weld. Res. Abroad*, 1995, **41**, (3), 29–31.
13. F. M. ELKIN, N. A. NARYSHKINA, V. N. ANAD'EV, and A. V. RUDOI: *Russ. Metall.*, (3), 110–115.
14. A. M. DRITZ and T. V. KRYMOVA: in Proc. 6th Int. Aluminum–Lithium Conf., Garmisch-Partenkirchen, Germany (ed. M. Peters and P.-J. Winkler), Vol. 2, 1233–1238; 1991, Oberursel, DGM Informationsgesellschaft.
15. I. N. FRIDLYANDER: *Met. Sci. Heat Treat.*, 1990, **32**, (4), 235–245.
16. J. R. PICKENS, F. H. HEUBAUM, T. J. LANGAN, and L. S. KRAMER: in Proc. 5th Int. Aluminum–Lithium Conf., Williamsburg, VA, (ed. T. H. Sanders and E. A. Starke), Vol. 3. 1397–1414; 1989, Edgbaston, Materials and Component Engineering Publ.
17. G. M. REDDY, A. A. GOKHALE, and K. PRASAD RAO: *Sci. Technol. Weld. Joining*, 1998, **3**, (3), 151–158.
18. J. C. LIPPOLD: 'A review of the physical metallurgy and welding characteristics of aluminum–lithium alloys', EWI project no. 3064, Edison Welding Institute, Columbus, OH, August 1987.
19. 'Metals handbook', 8th edn, Vol. 8; 1973, Westerville, OH, ASM.
20. H. M. FLOWER and P. J. GREGSON: *Mater. Sci. Technol.*, 1987, **3**, (2), 81–92.
21. D. B. WILLIAMS: in Proc. 1st Int. Aluminum–Lithium Conf., Stone Mountain, GA, (ed. T. H. Sanders and E. A. Starke), 89–100; 1981, Warrendale, PA, Metallurgical Society/AIME.
22. W. A. BAESLACK, III and K. H. HOU: *J. Mater. Sci. Lett.*, 1996, **15**, 239–244.
23. H. K. HARDY and J. M. SILCOCK: *J. Inst. Met.*, 1955–56, **84**, 423–428.
24. V. VLADMILOVIC and G. THOMAS: *J. Phys.*, 1987, **48**, C3-385–C3-396.
25. A. K. GUPTA, P. GAUNT, and M. C. CHATURVEDI: *Philos. Mag. A*, 1987, **55**, (3), 375–387.
26. D. W. LEVINSON and D. J. McPHERSON: *Trans. ASM*, 1956, **48**, 689–705.
27. V. I. ELAGIN, V. V. ZAKHAROV, and T. D. ROSTOVA: *Met. Sci. Heat Treat.*, 1992, **34**, (1–2), 37–45.
28. N. BLAKE and M. A. HOPKINS: *J. Mater. Sci.*, 1985, **20**, 2861–2867.
29. F. W. GAYLE and J. B. VANDERSANDE: *Scr. Metall.*, 1984, **18**, 473–478.
30. F. W. GAYLE and J. B. VANDERSANDE: in Proc. 3rd Int. Aluminium–Lithium Conf., (ed. C. Baker *et al.*), 509–515; 1986, Oxford, UK, Oxford University.
31. G. L. SHNEIDER and A. M. DRITS: *Met. Sci. Heat Treat.*, 1995, **37**, (9–10), 373–377.
32. C. KUMAI, J. KUSINSKI, G. THOMAS, and T. M. DEVINE: *Corrosion*, Apr. 1989, **45**, (4), 294–302.
33. I. N. FRIDLYANDER, V. S. SANDLER, and T. NIKOLOSKYA: *Met. Sci. Heat Treat.*, 1990, **32**, (6), 466–468.
34. E. S. BALMUTH and R. SCHMIDT: in Proc. 1st Int. Aluminum–Lithium Conf., Stone Mountain, GA, (ed. T. H. Sanders, Jr *et al.*), 69–88; 1981, Warrendale, PA, Metallurgical Society/AIME.
35. A. GYSLER, R. CROOKS, and E. A. STARKE: in Proc. 1st Int. Aluminum–Lithium Conf., (ed. T. H. Sanders, Jr *et al.*), 263–291; Warrendale, PA, TMS-AIME.
36. E. A. STARKE and F. S. LIN: *Metall. Trans. A*, Dec. 1982, **13**, 2259–2269.
37. J. D. BOYD and R. B. NICHOLSON: *Acta Metall.*, 1971, **19**, 1379–1391.
38. J. M. SILCOCK, T. J. HEAL, and H. K. HARDY: *J. Inst. Met.*, 1955–1956, **84**, 23–31.
39. F. S. LIN, S. B. CHAKRABORTTY, and E. A. STARKE: *Metall. Trans. A*, 1982, **13A**, 401–410.
40. T. H. SANDERS and E. A. STARKE: *Acta Metall.*, May 1982, **30**, (5), 927–939.
41. L. I. KAYGORODOVA, A. M. DRJTZ, T. V. KRYMOVA, and I. N. FRIDLYANDER: in Proc. 6th Int. Aluminum–Lithium Conf., Garmisch-Partenkirchen, Germany, (ed. M. Peters and P.-J. Winkler), Vol. 1, 363–367; 1991, Oberursel, DGM Informationsgesellschaft.
42. I. N. FRIDLYANDER, S. F. DANILOV, E. N. MALYSHEVA, T. A. GOROKHOVA, and N. N. KIRKINA: in Proc. 6th Int. Aluminum–Lithium Conf., Garmisch-Partenkirchen, Germany, (ed. M. Peters and P.-J. Winkler), Vol. 2, 381–386; 1991, Oberursel, DGM Informationsgesellschaft.
43. R. V. ILYUSHENKO, A. V. LOZOVSKAYA, I. E. SKLABINSKAYA, and E. O. PATON: in Proc. 6th Int. Aluminum–Lithium Conf., Garmisch-Partenkirchen, Germany, (ed. M. Peters and P.-J. Winkler), Vol. 2, 1251–1256; 1991, Oberursel, DGM Informationsgesellschaft.
44. K. H. HOU and W. A. BAESLACK: *J. Mater. Sci. Lett.*, 1996, **15**, 208–213.
45. R. P. MARTUKANITZ and P. R. HOWELL: 'Relationships involving process, microstructure, and properties of weldments of Al–Cu and Al–Cu–Li alloys', submitted to Proc. Conf. 'World trends in welding research'; 1996, Westerville, OH, ASM International.
46. S. D. DUMOLT: 'An investigation of the microstructural changes in the heat affected zone of age hardenable aluminum alloys

using transmission electron microscopy', PhD dissertation, Carnegie-Mellon University, Pittsburg, PA, July 1983.
47. J. R. PICKENS, T. L. LANGAN, and E. BARTA: in Proc. 3rd Int. Aluminum–Lithium Conf., (ed. C. Baker *et al.*), 137–147; 1985, Oxford, UK, University of Oxford.
48. S. J. SUNWOO and J. W. MORRIS: *Weld. J.*, 1989, **68**, 262s–268s.
49. S. J. SUNWOO, E. L. BRADLEY, and J. W. MORRIS: *Metall. Trans. A*, Oct. 1990, **21A**, (10), 2795–2804.
50. C. E. CROSS, L. W. LOECHEL, and G. F. BRAUN: in Proc. 6th Int. Aluminum–Lithium Conf., Garmisch-Partenkirchen, Germany, (ed. M. Peters and P.-J. Winkler), Vol. 2, 1165–1170; 1991, Oberursel, DGM Informationsgesellschaft.
51. M. F. GITTOS: 'The application of resistance and laser welding to the Al–Li alloy 8090', TWI research report, May 1990.
52. V. I. RYAZANTSEV *et al.*: *Weld. Prod.*, 1977, **24**, (4), 21–26.
53. C. J. DAWES and W. M. THOMAS: *Weld. J.*, Mar. 1996, **75**, (3), 41–45.
54. P. J. DITZEL: 'Microstructure property relationships in aluminum friction stir welds', masters thesis, The Ohio State University, 1997.
55. J. C. LIPPOLD and W. LIN: in Proc. 5th Int. Conf. on Aluminum Alloys, Grenoble, France, 1–5 July 1996, (ed. J. H. Driver *et al.*), 1685–1690; 1996, Zeurich-Uetikon, Switzerland, Trans Tech Publ.
56. L. S. KRAMER, C. E. CROSS, and J. R. PICKENS: in Proc. 6th Int. Aluminum–Lithium Conf., Garmisch-Partenkirchen, Germany, (ed. M. Peters and P.-J. Winkler), Vol. 2, 1197–1202; 1991, Oberursel, DGM Informationsgesellschaft.
57. C. E. CROSS, D. L. OLSON, G. R. EDWARDS, and J. F. CAPES: 'Aluminum–lithium alloys II', (ed. E. A. Starke and T. H. Sanders), 675–682; 1983, TMS/AIME.
58. W. I. PUMPHREY and J. V. LYONS: *J. Inst. Met.*, 1948, **75**, 439–455.
59. W. KURZ and D. J. FISHER: 'Fundamentals of solidification', 3rd edn, 1992, Aedermannsdorf, Switzerland, Trans Tech Publ.
60. L. S. KRAMER, F. H. HEUBAUM, and J. R. PICKENS: in Proc. 5th Int. Aluminum–Lithium Conf., Williamsburg, VA, (ed. T. H. Sanders and E. A. Starke), Vol. III, 1415–1424; 1989, Edgbaston, Materials and Component Engineering Publ.
61. M. F. GITTOS: in Proc. Int. Conf. Advanced Aluminium and Magnesium Alloys, Amsterdam, The Netherlands, 181–188; 1990, Materials Park, OH, ASM.
62. W. I. PUMPHREY and D. C. MOORE: *J. Inst. Met.*, 1948, **75**, 425–438.
63. C. E. CROSS, W. T. TACK, L. W. LOECHEL, and L. S. KRAMER: in Proc. Materials Weldability Symp., Detroit, MI, 275–282; 1990, Materials Park, OH, ASM.
64. W. LIN: 'A methodology of quantifying heat-affected zone liquation cracking susceptibility', PhD thesis, The Ohio State University, 1991.
65. T. ZACHARIA, S. A. DAVID, J. M. VITEK, and R. P. MARTUKANITZ: in Proc. 5th Int. Aluminum–Lithium Conf., Williamsburg, VA, (ed. T. H. Sanders and E. A. Starke), Vol. III, 1387–1396; 1989, Edgbaston, Materials and Component Engineering Publ.
66. H. YUNJIA, G. DALU, and S. ZHIXIONG: in Proc. 6th Int. Aluminum–Lithium Conf., Garmisch-Partenkirchen, Germany, (ed. M. Peters and P.-J. Winkler), Vol. 2, 1215–1220; 1991, Oberursel, DGM Informationsgesellschaft.
67. H. YUNJIA, G. DALU, and S. ZHIXIONG: in Proc. 6th Int. Aluminum–Lithium Conf., Garmisch-Partenkirchen, Germany, (ed. M. Peters and P.-J. Winkler), Vol. 2, 1203–1208; 1991, Obersursel, DGM Informationsgesellschaft.
68. S. R. SHAH, J. E. WITTIG, and G. T. HAHN: 'International trends in welding science and technology', 281–285; 1993, Westerville, OH, ASM.
69. A. E. GUTIERREZ, J. C. LIPPOLD, and W. LIN: in Proc. 5th Int. Conf. Aluminum Alloys, Grenoble, France, (ed. J. H. Driver *et al.*), 1691–1696; 1996, Zeurich-Uetikon, Switzerland, Trans Tech Publ.
70. A. E. GUTIERREZ and J. C. LIPPOLD: *Weld. J.*, 1998, **77**, (3), 123-s.
71. A. KOSTRIVAS and J. C. LIPPOLD: unpublished research ongoing at The Ohio State University, 1998.
72. R. P. MARTUKANITZ, C. A. NATALIE, and J. O. KNOEFEL: *J. Met.*, 1987, **39**, (11), 38–42.
73. M. R. EDWARDS and V. E. STONEHAM: *J. Phys.*, 1987, **48**, (9), C3.293–C3.299.
74. V. N. MIRONENKO, V. S. EVSTIFEEV, G. I. LUBENETS, S. A. KORSHUNKOVA, V. V. ZAKHAROV, and A. I. LITVINTSEV: *Weld. Prod.*, 1979, **26**, (1), 30–31.
75. P. A. MOLIAN and T. S. SRIVATSAN: in Proc. 5th Int. Aluminum–Lithium Conf., Williamsburg, VA, (ed. T. H. Sanders and E. A. Starke), Vol. III, 1435–1445; 1989, Edgbaston, Materials and Component Engineering Publ.
76. T. A. MARISCO and R. KOSSOWSKY: in Proc. 5th Int. Aluminum–Lithium Conf., Williamsburg, VA, (ed. T. H. Sanders and E. A. Starke), Vol. III, 1447–1456; 1989, Edgbaston, Materials and Component Engineering Publ.
77. M. J. PARZUCHOWSKI, E. J. TUEGEL, and K. K. SANKARAN: in Proc. 6th Int. Aluminum–Lithium Conf., Garmisch-Partenkirchen, Germany, (ed. M. Peters and P.-J. Winkler), Vol. 2, 777–782; 1991, Oberursel, DGM Informationsgesellschaft.
78. Z. YUN, L. YULIN, Z. HONGEN, H. ZANGQI, Z. ZHIYONG, W. XINGHUA, and W. ZENFU: in Proc. 6th Int. Aluminum–Lithium Conf., Garmisch-Partenkirchen, Germany, (ed. M. Peters and P.-J. Winkler), Vol. 2, 819–824; 1991, Oberursel, DGM Informationsgesellschaft.
79. B. BAVARIAN, J. BECKER, S. N. PARIKH, and M. ZAMANZADEH: in Proc. 5th Int. Aluminium–Lithium Conf., Williamsburg, VA, (ed. T. H. Sanders and E. A. Starke), Vol. III, 1227–1236; 1989, Edgbaston, Materials and Component Engineering Publ.
80. T. S. SRIVATSAN, G. E. BOBECK, T. S. SURDARSHAN, and P. A. MOLIAN: in Proc. 5th Int. Aluminium–Lithium Conf., Williamsburg, VA, (ed. T. H. Sanders and E. A. Starke), Vol. III, 1237–1249; 1989, Edgbaston, Materials and Component Engineering Publ.
81. K. MOORE, T. J. LANGAN, F. H. HEUBAUM, and J. R. PICKENS: in Proc. 5th Int. Aluminium–Lithium Conf., Williamsburg, VA, (ed. T. H. Sanders and E. A. Starke), Vol. III, 1281–1291; 1989, Edgbaston, Materials and Component Engineering Publ.
82. R. BALASUBRAMANIAM, D. J. DUQUETTE, and K. RAJAN: *Acta Metall. Mater.*, 1991, **39**, (11), 2597–2605.
83. P. N. ANYALEBECHI, D. E. J. TALBOT, and D. A. GRANGER: *Metall. Trans. B*, 1989, **20B**, 523–533.
84. R. G. BUCHHEIT, F. D. WALL, G. E. STONER, and J. P. MORAN: *Corrosion*, 1995, **51**, (6), 417–428.
85. W. N. GARRAD: *Corrosion*, 1994, **50**, (3), 215–225.
86. D. WEBSTER and C. G. BENNET: 'Tough(er) aluminum–lithium alloys', *Adv. Mater. Process.*, 1989, **136**, (4), 49–54.